PHYSICAL REVIEW B **82**, 134521 (2010)

Non-Abelian topological orders and Majorana fermions in spin-singlet superconductors

Masatoshi Sato,[1] Yoshiro Takahashi,[2] and Satoshi Fujimoto[2]
[1]*The Institute for Solid State Physics, The University of Tokyo, Kashiwanoha 5-1-5, Kashiwa-shi, Chiba 277-8581, Japan*
[2]*Department of Physics, Kyoto University, Kyoto 606-8502, Japan*
(Received 24 June 2010; revised manuscript received 9 September 2010; published 18 October 2010)

The non-Abelian topological order for superconductors is characterized by the existence of zero-energy Majorana fermions in edges of systems and in a vortex of a macroscopic condensate, which obey the non-Abelian statistics. This paper is devoted to an extensive study on the non-Abelian topological phase of spin-singlet superconductors with the Rashba spin-orbit interaction proposed in our previous paper [M. Sato, Y. Takahashi, and S. Fujimoto, Phys. Rev. Lett. **103**, 020401 (2009)]. We mainly consider the *s*-wave pairing state and the $d+id$ pairing state. In the case of $d+id$-wave pairing, Majorana fermions appear in almost all parameter regions of the mixed state under an applied magnetic field, provided that the Fermi level crosses k points in the vicinity of the Γ point or the M point in the Brillouin zone while in the case of *s*-wave pairing, a strong magnetic field, the Zeeman energy of which is larger than the superconducting gap is required to realize the topological phase. We clarify that Majorana fermions in Rashba spin-singlet superconductors are much more stable than those realized in spin-triplet $p+ip$ superconductors in certain parameter regions. We also investigate the topological number which ensures the topological stability of the phase in detail. Furthermore, as a by-product, we found that topological order is also realized in conventional spin (or charge)-density wave states with the Rashba spin-orbit interaction, for which massless Dirac fermions appear in the edge of the systems and charge fractionalization occurs.

DOI: 10.1103/PhysRevB.82.134521 PACS number(s): 74.90.+n, 03.65.Vf, 71.10.Pm, 67.85.−d

I. INTRODUCTION

Topological states of condensed-matter systems are characterized by a bulk topological number such as the Chern number [or the Thouless-Kohmoto-Nightingale-Nijs (TKNN) number] which represents a topologically nontrivial structure of the many-body Hilbert space. In such phases, topologically protected surface states and fractionalized quasiparticles, e.g., anyons, appear.[1–11] In particular, when topological order is realized in a certain class of superconductors, this topological phase supports the existence of chiral Majorana edge modes and a Majorana fermion in a vortex core.[3–9] Vortices with Majorana fermion modes are neither fermions nor bosons but non-Abelian anyons, obeying the non-Abelian statistics for which the exchange operations of particles are not commutative.[3–8] Because of this remarkable feature, a vortex with a Majorana fermion may be utilized as a decoherence-free qubit, and plays an important role for the realization of fault-tolerant topological quantum computation.[12–14] The state with non-Abelian anyons, which is called the non-Abelian topological phase, has been discussed to be realized in the fractional quantum Hall effect state with $\nu=5/2$ and 12/5.[3–5,15] It has been also known that spin-triplet superconductors such as chiral $p+ip$ superconductors,[6,7,16–20] and noncentrosymmetric (NCS) *p*-wave superconductors with broken time-reversal symmetry,[21] possess a zero-energy Majorana mode, and realizes a non-Abelian topological phase. In general, fully gapped spin-triplet superconductors support non-Abelian anyons if the number of the connected Fermi surfaces are odd, in the case without time-reversal symmetry.[22] For the spin-singlet *s*-wave superconducting state, it was pointed out by Fu and Kane that non-Abelian anyons are realized in the proximity with a topological insulator.[23] Also, the non-Abelian anyons in the *s*-wave pairing state was discussed before in the context of axion strings in cosmological systems.[24,25]

Recently, the present authors proposed another scenario of a non-Abelian topological phase in NCS *s*-wave superfluids or superconductors. We pointed out that in the presence of the Rashba spin-orbit (SO) interaction, *s*-wave superconducting states show a transition to the non-Abelian topological phase with nonzero Chern number, under an applied strong Zeeman magnetic field.[26] Also, independently, it was proposed by Sau *et al.*[27] that such systems can be realized in heterostructure semiconductor devices. The idea was subsequently generalized by Alicea.[28]

In this paper, we explore extensively properties of the non-Abelian topological phase realized in NCS spin-singlet superconductors with the Rashba SO interaction, which was considered in our previous paper.[26] There are two main purposes. The first one is to present the detail analysis of chiral Majorana edge states and a Majorana fermion mode in a vortex core in the case of the NCS *s*-wave superconductor, and the calculation of the topological number, which are omitted in Ref. 26. The topological order for time-reversal symmetry broken (TRB) systems in two dimensions (2D) is characterized by the first Chern number. We present a formulation for the calculation of the Chern number with the use of a winding number, which makes the estimation of the topological number easier. Using this formulation, we explore the non-Abelian topological order realized in NCS spin-singlet superconductors. We, furthermore, analyze the vortex core state by solving the Bogoliubov-de Gennes (BdG) equation. We obtain the zero-energy Majorana fermion solution when the Zeeman energy due to an applied magnetic field is larger than the superconducting gap Δ. We also discuss that, in some parameter regions, the Majorana fermion in NCS spin-

singlet superconductors is remarkably stable compared to that in chiral $p+ip$ superconductors. This feature is crucially important for the application to the topological quantum computation. The superior stability of Majorana mode in a vortex core of NCS spin-singlet superconductors stems from the fact that when the Zeeman energy $\mu_B H_z$ satisfies the condition $\Delta > \mu_B H_z - \Delta > 0$, the Majorana fermion is mainly formed by the superposition of quasiparticles in the vicinity of the Γ point (or the M point) with the Fermi momentum $\mathbf{k}_F \sim 0$ [or (π, π)], in the long-distance asymptotic regime sufficiently far from the center of the vortex core. Because of this property, the excitation energy E_0 in a vortex core which separates the zero-energy Majorana mode and the first excited state is much larger than a typical energy scale of the Andreev bound state of vortex cores $\sim \Delta^2 / E_F$. Furthermore, the vanishing Fermi momentum for a Majorana fermion implies that decoherence due to quantum oscillations of quasiparticle energy with a period $\sim 1/k_F$ raised by intervortex tunneling,[29] which may be an obstruction for the implementation of the topological quantum computation, is substantially suppressed.

The second purpose of this paper is to extend the scenario of the non-Abelian topological order for the case of s-wave pairing state to other spin-singlet pairing states. In particular, we consider the cases of $d+id$-wave pairing, for which there is a full gap in the energy spectrum, ensuring the nonzero Chern number. It is demonstrated that in the $d+id$-wave pairing state with the Rashba SO interaction, when the Fermi level crosses k points in the vicinity of the Γ point or the M point in the Brillouin zone (BZ), the non-Abelian topological order, which supports the existence of chiral Majorana edge states and a Majorana fermion mode in a vortex core, appears under an applied magnetic field. In contrast to the case of s-wave pairing considered in Refs. 26–28, for which Majorana fermions appear only when there is Zeeman splitting larger than the superconducting gap, a small magnetic field larger than the lower critical field suffices for the realization of the non-Abelian topological order in the $d+id$-wave pairing state. Thus, it may be easier to realize Majorana fermions in the NCS $d+id$-wave superconductor than in the NCS s-wave superconductor.

Furthermore, we consider another direction of the extension of the scenario for the non-Abelian topological order. Our results for Rashba s-wave superconductors imply that the topological order is also realizable in the conventional spin-density wave (SDW) state or the charge-density wave (CDW) state with the Rashba SO interaction. We demonstrate that in these density wave states, the Abelian topological order appear under applied magnetic fields, leading to the existence of gapless edge states described by the Dirac fermion, which is analogous to the surface states of the topological insulator. We also discuss the scenario of charge fractionalization in the topological density wave states.

The organization of this paper is as follows. From Sec. II to Sec. III, we introduce the model for superconductors with the Rashba SO interaction in two dimensions, upon which our analysis is focused, and, as a first step of our analysis, classify the parameter regions of the model, in which different topological phases may be realized. In Sec. IV, we explain the duality relation which holds for our model Hamiltonian. This duality relation was utilized for the analysis of topological properties in Ref. 26. In the most part of this paper, we do not use the duality relation but instead, confirm the argument based on it developed in Ref. 26 by adopting a more direct approach to this issue. In Sec. V, we analyze and discuss the topological number characterizing the non-Abelian topological phases realized in NCS spin-singlet superconductors. In particular, we prove the relation between the Chern number and the winding number, which is useful for the investigation of the topological order. Using this relation, we elucidate the general condition for the realization of the non-Abelian topological order. On the basis of the analysis of the topological number, we obtain the phase diagram of the topological order for spin-singlet NCS superconductors. We also give some physical arguments on the origin of the topological order in spin-singlet NCS superconductors. In Sec. VI, the numerical results for chiral Majorana edge modes are presented for the cases of s-wave pairing and $d+id$-wave pairing. In Sec. VII, we consider an approximated but analytical solution of the BdG equation for Majorana zero-energy modes in vortex cores. We, also, discuss the superior stability of the Majorana mode in NCS spin-singlet superconductors compared to that in chiral $p+ip$ superconductors. In Sec. VIII, topological density wave states in which gapless Dirac fermions on the edge of systems appear and charge fractionalization occurs are considered. In Sec. IX, we give a summary of our results and also discuss possible realization of the NCS spin-singlet superconductors with the non-Abelian topological order in real systems.

Some technical details are presented in Appendices. In Appendices A and B, we derive useful formulas for the Chern numbers and the winding numbers, which were used for the discussion on the topological number in Sec. V. Supplementary discussions related to the topological argument given in Sec. V are presented in Appendix C. The details of the derivation of the BdG equation for a singlet vortex are given in Appendix D. In Appendix E, we discuss another mechanism of non-Abelian anyons in spin-singlet superconductors, which was first discussed in Ref. 24, where non-Abelian anyons are realized in time-reversal invariant s-wave superconducting state without a Zeeman magnetic field. This discussion is relevant to the non-Abelian topological order realized in an interface between an s-wave superconductor and a time-reversal invariant topological insulator proposed by Fu and Kane.[23]

II. MODEL

In this paper, we consider spin-singlet superconductors with the Rashba SO interaction[30] in two dimensions. For concreteness, we define our model in the square lattice while the following argument does not rely on the particular choice of the crystal structure. It is also noted that our analysis and results are also generalized straightforwardly to other type of antisymmetric SO interactions raised by the lack of inversion center of systems. The Hamiltonian is given by

$$\mathcal{H} = \sum_{\mathbf{k},\sigma} \varepsilon(\mathbf{k}) c^{\dagger}_{\mathbf{k}\sigma} c_{\mathbf{k}\sigma} - \mu_B H_z \sum_{\mathbf{k},\sigma,\sigma'} (\sigma_z)_{\sigma\sigma'} c^{\dagger}_{\mathbf{k}\sigma} c_{\mathbf{k}\sigma'} + \alpha \sum_{\mathbf{k},\sigma,\sigma'} \mathcal{L}_0(\mathbf{k}) \cdot \boldsymbol{\sigma}_{\sigma\sigma'} c^{\dagger}_{\mathbf{k}\sigma} c_{\mathbf{k}\sigma'} + \frac{1}{2} \sum_{\mathbf{k},\sigma,\sigma'} \Delta_{\sigma\sigma'}(\mathbf{k}) c^{\dagger}_{\mathbf{k}\sigma} c^{\dagger}_{-\mathbf{k}\sigma'} + \frac{1}{2} \sum_{\mathbf{k},\sigma,\sigma'} \Delta^{*}_{\sigma'\sigma}(\mathbf{k}) c_{-\mathbf{k}\sigma} c_{\mathbf{k}\sigma'}, \tag{1}$$

where $c^{\dagger}_{\mathbf{k}\sigma}$ ($c_{\mathbf{k}\sigma}$) is a creation (an annihilation) operator for an electron with momentum $\mathbf{k}=(k_x,k_y)$, spin σ. The energy-band dispersion is $\varepsilon(\mathbf{k})=-2t(\cos k_x+\cos k_y)-\mu$ with the hopping parameter t and the chemical potential μ, and the Rashba SO coupling is $\alpha\mathcal{L}_0(\mathbf{k})=\alpha(\sin k_y,-\sin k_x)$ $(\alpha>0)$. We also introduce the Zeeman coupling $-\mu_B H_z \Sigma_{\mathbf{k},\sigma\sigma'}(\sigma_z)_{\sigma\sigma'} c^{\dagger}_{\mathbf{k}\sigma} c_{\mathbf{k}\sigma'}$ in the Hamiltonian.

For the spin-singlet superconductors, the gap function $\Delta_{\sigma\sigma'}(\mathbf{k})$ is written as

$$\Delta_{\sigma\sigma'}(\mathbf{k}) = i\Delta(\mathbf{k})(\sigma_y)_{\sigma\sigma'} \tag{2}$$

with the y component of the Pauli matrices σ_i $(i=x,y,z)$. In the following, we assume two different full-gapped spin-singlet superconductors: the first one is the s-wave pairing, $\Delta(\mathbf{k})=\Delta_s$, and the other is the $d+id$-wave pairing. For the $d+id$ pairing, we consider two possible realization on the lattice, $\Delta(\mathbf{k})=\Delta_d^{(1)}(\cos k_y-\cos k_x)+i\Delta_d^{(2)} \sin k_x \sin k_y$ or $\Delta(\mathbf{k})=\Delta_d^{(1)}(\sin^2 k_x-\sin^2 k_y)+i\Delta_d^{(2)} \sin k_x \sin k_y$. The amplitudes Δ_s and $\Delta_d^{(i)}$ $(i=1,2)$ are chosen as real and positive. The second type of the $d+id$-wave pairing includes higher harmonic contributions, which may arise depending on detailed structures of electronic bands and the pairing interactions. We use these two types of the $d+id$-wave gap to clarify that, although both of them support the non-Abelian topological order, the precise condition for the non-Abelian phase slightly depends on the detail of the gap structure.

For a noncentrosymmetric superconductor, the parity mixing of the gap function generally occurs.[31–35] Therefore, in addition to the spin-singlet component of the gap function, the spin-triplet one is induced generally. However, if the spin-singlet amplitude dominates the gap function, the topological nature is not affected by the spin-triplet one. We neglect the spin-triplet component in the following.

In the following, we mainly consider the case that SO interaction is much larger than the Zeeman energy; i.e., $\alpha|\mathcal{L}_0(\mathbf{k})| \gg \mu_B H_z$, which is an important condition for the stability of the superconducting state against the Pauli depairing effect due to the magnetic fields.

III. GAP CLOSING CONDITION

In general, continuous topological phase transitions between topologically distinct phases occur only when the energy gap of the bulk spectrum closes. Thus, to identify parameter regions for which different topological phases are realized, we first examine the bulk spectrum of the system. To obtain the bulk spectrum, we rewrite the Hamiltonian as

$$\mathcal{H} = \frac{1}{2} \sum_{\mathbf{k},\sigma,\sigma'} (c^{\dagger}_{\mathbf{k}\sigma}, \quad c_{-\mathbf{k}\sigma}) \mathcal{H}(\mathbf{k}) \begin{pmatrix} c_{\mathbf{k}\sigma'} \\ c^{\dagger}_{-\mathbf{k}\sigma'} \end{pmatrix}, \tag{3}$$

where the BdG Hamiltonian $\mathcal{H}(\mathbf{k})$ is given by

$$\mathcal{H}(\mathbf{k}) = \begin{pmatrix} \varepsilon(\mathbf{k}) - \mu_B H_z \sigma_z + \alpha \mathcal{L}_0(\mathbf{k}) \cdot \boldsymbol{\sigma} & i\Delta(\mathbf{k})\sigma_y \\ -i\Delta(\mathbf{k})^{*}\sigma_y & -\varepsilon(\mathbf{k}) + \mu_B H_z \sigma_z + \alpha \mathcal{L}_0(\mathbf{k}) \cdot \boldsymbol{\sigma}^{*} \end{pmatrix}. \tag{4}$$

Diagonalizing the BdG Hamiltonian, we find

$$E(\mathbf{k}) = \sqrt{\varepsilon(\mathbf{k})^2 + \alpha^2 \mathcal{L}_0(\mathbf{k})^2 + \mu_B^2 H_z^2 + |\Delta(\mathbf{k})|^2 \pm 2\sqrt{\varepsilon(\mathbf{k})^2 \alpha^2 \mathcal{L}_0(\mathbf{k})^2 + [\varepsilon(\mathbf{k})^2 + |\Delta(\mathbf{k})|^2]\mu_B^2 H_z^2}}. \tag{5}$$

In our model, the gap of the system closes only when the following condition is satisfied:

$$\varepsilon(\mathbf{k})^2 + \alpha^2 \mathcal{L}_0(\mathbf{k})^2 + \mu_B^2 H_z^2 + |\Delta(\mathbf{k})|^2 = 2\sqrt{\varepsilon(\mathbf{k})^2 \alpha^2 \mathcal{L}_0(\mathbf{k})^2 + [\varepsilon(\mathbf{k})^2 + |\Delta(\mathbf{k})|^2]\mu_B^2 H_z^2}. \tag{6}$$

From a straightforward calculation,[36] it is found that this condition is equivalent to

$$\varepsilon(\mathbf{k})^2 + |\Delta(\mathbf{k})|^2 = \mu_B^2 H_z^2 + \alpha^2 \mathcal{L}_0(\mathbf{k})^2, \quad |\Delta(\mathbf{k})|\alpha\mathcal{L}_0(\mathbf{k}) = 0. \tag{7}$$

We examine the gap closing condition using Eq. (7) for the s-wave pairing state and the $d+id$-wave pairing state in the following.

A. s-wave Rashba superconductor

For the s-wave pairing, the second equation in Eq. (7) is met only when $\mathcal{L}_0(\mathbf{k})=0$. Therefore, the gap closes at $\mathbf{k}=(0,0),(0,\pi),(\pi,0),(\pi,\pi)$. Substituting those values into the first equation in Eq. (7), we have three different gap closing conditions [in the square lattice, the condition at $\mathbf{k}=(\pi,0)$ and that at $\mathbf{k}=(0,\pi)$ are the same, so we have only three conditions],

$$(4t+\mu)^2 + \Delta_s^2 = (\mu_B H_z)^2, \quad \mu^2 + \Delta_s^2 = (\mu_B H_z)^2, \quad (4t-\mu)^2 + \Delta_s^2 = (\mu_B H_z)^2. \tag{8}$$

When one of these Eq. (8) is satisfied, the energy gap closes. From these conditions, we find that there are at least seven

regions of parameter space, which may be topologically distinct, as shown in Fig. 1. We will explore the topological numbers associated with these different regions and classify the topological phases of our system in Sec. V.

B. $d+id$-wave Rashba superconductor

1. Case of $\Delta(\mathbf{k})=\Delta_d^{(1)}(\cos k_y-\cos k_x)+i\Delta_d^{(2)}\sin k_x\sin k_y$

For this $d+id$-wave gap, the second equation in Eq. (7) is met either when $\mathcal{L}_0(\mathbf{k})=0$ or when $\Delta(\mathbf{k})=0$. This condition is satisfied at $\mathbf{k}=(0,0),(\pi,0),(0,\pi),(\pi,\pi)$. Substituting these $\mathbf{k}$s′ in the first equation in Eq. (7), we have

$$(4t+\mu)^2=(\mu_B H_z)^2,\quad \mu^2+4(\Delta_d^{(1)})^2=(\mu_B H_z)^2,\qquad (9)$$

$$(4t-\mu)^2=(\mu_B H_z)^2.$$

The conditions obtained here are very similar to those for s-wave pairing. However, there is an important difference between them. The first and the last equations of the gap closing condition [Eq. (9)] do not depend on the amplitude of the pairing gap. Because of this feature, even for a relatively weak Zeeman field where the orbital depairing effect is negligible, the gap can close, and the topological phase transition occurs, provided that the chemical potential μ is properly tuned as $\mu\sim\pm 4t$. As will be seen later, this point is crucially important for the feasibility of the realization of the non-Abelian topological order in the $d+id$-wave pairing case, compared to the s-wave pairing state.

2. Case of $\Delta(\mathbf{k})=\Delta_d^{(1)}(\sin^2 k_x-\sin^2 k_y)+i\Delta_d^{(2)}\sin k_x\sin k_y$

As in the previous case, the second equation in Eq. (7) is met either when $\mathcal{L}_0(\mathbf{k})=0$ or when $\Delta(\mathbf{k})=0$. Accidently, both of them are satisfied at the same momenta $\mathbf{k}=(0,0),(0,\pi),(\pi,0),(\pi,\pi)$. Substituting those values into the first equation in Eq. (7), we have

$$(4t+\mu)^2=(\mu_B H_z)^2,\quad \mu^2=(\mu_B H_z)^2,\quad (4t-\mu)^2=(\mu_B H_z)^2. \qquad (10)$$

In this case, all of the gap closing conditions [Eq. (10)] do not depend on the pairing gap, and thus, the topological phase transition can occur even for a weak magnetic field for $\mu\sim\pm 4t,0$. The difference between the second equation of Eq. (9) and that of Eq. (10) yields a slight difference of the parameter regions where a topological order occurs.

IV. DUALITY RELATION IN BdG HAMILTONIAN

As discussed in Ref. 26, an underlying mechanism of the realization of the non-Abelian topological order in the Rashba s-wave superconductor is understood in terms of the duality relation satisfied by model (1); i.e., the BdG Hamiltonian $\mathcal{H}(\mathbf{k})$ is unitary equivalent to the following dual Hamiltonian $\mathcal{H}_D(\mathbf{k})$:

$$\mathcal{H}_D(\mathbf{k})=D\mathcal{H}(\mathbf{k})D^\dagger=\begin{pmatrix}\mathrm{Re}\,\Delta(\mathbf{k})-\mu_B H_z\sigma_z & -i[\varepsilon(\mathbf{k})-i\,\mathrm{Im}\,\Delta(\mathbf{k})]\sigma_y-i\alpha\mathcal{L}_0(\mathbf{k})\cdot\boldsymbol{\sigma}\sigma_y\\ i[\varepsilon(\mathbf{k})+i\,\mathrm{Im}\,\Delta(\mathbf{k})]\sigma_y+i\alpha\mathcal{L}_0(\mathbf{k})\sigma_y\cdot\boldsymbol{\sigma} & -\mathrm{Re}\,\Delta(\mathbf{k})+\mu_B H_z\sigma_z\end{pmatrix}, \qquad (11)$$

where D is the constant unitary matrix given by

$$D=\frac{1}{\sqrt{2}}\begin{pmatrix}1 & i\sigma_y\\ i\sigma_y & 1\end{pmatrix}. \qquad (12)$$

As is shown in Appendix A, the dual transformation accomplished by the constant unitary matrix does not change the first Chern number of the system. Therefore, the original Hamiltonian has the same topological properties as the dual one.

It should be remarked here that the Rashba spin-orbit interaction $\alpha\mathcal{L}_0(\mathbf{k})\cdot\boldsymbol{\sigma}$ in the original BdG Hamiltonian $\mathcal{H}(\mathbf{k})$ induces "the p-wave gap function" $-\alpha\mathcal{L}_0(\mathbf{k})\cdot\boldsymbol{\sigma}\sigma_y$ in the dual BdG Hamiltonian. However, this does not necessary means that the topological properties of our system is the same as those of a p-wave superconductor since $\mathcal{H}_D(\mathbf{k})$ has a nonstandard kinetic term given by $\mathrm{Re}\,\Delta_s(\mathbf{k})$. Nevertheless, we will show in the following sections that the topological order similar to a chiral $p+ip$-wave superconductor emerges under a large Zeeman field. Furthermore, the topological order in our system is much more robust than that of a chiral $p+ip$-wave superconductor.

In the most part of this paper, we do not use the dual Hamiltonian $\mathcal{H}_D(\mathbf{k})$, but, instead, analyze the original Hamiltonian $\mathcal{H}(\mathbf{k})$ directly. Our analysis using $\mathcal{H}(\mathbf{k})$ in this paper confirm the correctness of the argument based on the dual Hamiltonian developed in Ref. 26.

V. TOPOLOGICAL NUMBERS

As a conventional long-range order such as magnetic order is characterized by the existence of a nonzero local order parameter, a topological phase is also specified by a characteristic quantity similar to an order parameter; this is a topological number. In this section, we evaluate the topological number characterizing the non-Abelian topological order realized in Rashba spin-singlet superconductors.

For two-dimensional TRB superconductors, on which our discussion is focused, an important topological number is the TKNN number (equivalent to the first Chern number) I_{TKNN}, which is defined as follows. Let us consider the BdG equation

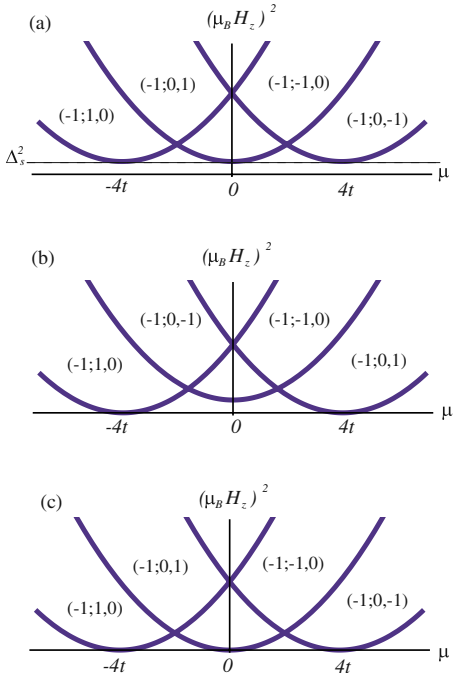

FIG. 1. (Color online) The diagrams of the non-Abelian topological phase for spin-singlet NCS superconductors. (a) *s*-wave case. (b) $d+id$-wave case with $\Delta(\mathbf{k})=\Delta_d^{(1)}(\cos k_y-\cos k_x)+i\Delta_d^{(2)}\sin k_x\sin k_y$. (c) $d+id$-wave case with $\Delta(\mathbf{k})=\Delta_d^{(1)}(\sin^2 k_x-\sin^2 k_y)+i\Delta_d^{(2)}\sin k_x\sin k_y$. The topological numbers $((-1)^{\nu_{\mathrm{Ch}}};I(0),I(\pi))$ are given only in the phases supporting a non-Abelian topological order. In each case, there are four different non-Abelian topological phases. In the *s*-wave case, the non-Abelian topological phase is realized only when the Zeeman magnetic field satisfies $(\mu_B H_z)^2>(\Delta_s)^2$ but in the $d+id$-wave cases, the non-Abelian topological phase can be realized even for a small but nonzero H_z.

$$\mathcal{H}(\mathbf{k})|\phi_n(\mathbf{k})\rangle = E_n(\mathbf{k})|\phi_n(\mathbf{k})\rangle. \tag{13}$$

By using the normalized occupied states, "the gauge field" $A_i^{(-)}(\mathbf{k})$ is defined as

$$A_i^{(-)}(\mathbf{k}) = i\sum_{E_n<0}\langle\phi_n(\mathbf{k})|\partial_{k_i}\phi_n(\mathbf{k})\rangle. \tag{14}$$

Then the TKNN number is given by

$$I_{\mathrm{TKNN}} = \frac{1}{2\pi}\int_{T^2} dk_x dk_y \mathcal{F}^{(-)}(\mathbf{k}), \tag{15}$$

where T^2 is the first Brillouin zone in the momentum space, $\mathcal{F}^{(-)}(\mathbf{k})$ is the "field strength of the gauge field" $A_i^{(-)}(\mathbf{k})$, that is, $\mathcal{F}^{(-)}(\mathbf{k})=\epsilon^{ij}\partial_{k_i}A_j^{(-)}(\mathbf{k})$.

The nonzero TKNN number implies the existence of topological order in the system under consideration. In general, the nonzero TKNN number allows both the Abelian topological order, for which there are no non-Abelian anyons, and the non-Abelian topological order, which is characterized by the non-Abelian statistics. For the Rashba superconductor, the Hamiltonian of which Eq. (4) is a 4×4 matrix, we can calculate I_{TKNN} directly from the above equations. However, here, we exploit a different method for the evaluation of the topological number, which is practically easier to be carried out. Furthermore, this method is quite useful for the elucidation of the realization of the non-Abelian topological order. A key idea of our method is to utilize another topological number specific to the Rashba superconductors, which is called the winding number.[21]

The winding number is introduced as follows.[21] Let us consider the particle-hole symmetry of the BdG Hamiltonian,

$$\Gamma\mathcal{H}(\mathbf{k})\Gamma^\dagger = -\mathcal{H}^*(-\mathbf{k}), \tag{16}$$

where Γ is given by

$$\Gamma = \begin{pmatrix} 0 & 1_{2\times2} \\ 1_{2\times2} & 0 \end{pmatrix}. \tag{17}$$

For $k_y=0$ or π, it is found that the BdG Hamiltonian (4) of our model satisfies $\mathcal{H}^*(-\mathbf{k})=\mathcal{H}(\mathbf{k})$. Thus the particle-hole symmetry yields that

$$[\Gamma,\mathcal{H}(\mathbf{k})]_+ = 0 \tag{18}$$

for $k_y=0,\pi$. From this relation, it is found that if we take the basis where Γ has the diagonal form as

$$\Gamma = \begin{pmatrix} 1_{2\times2} & 0 \\ 0 & -1_{2\times2} \end{pmatrix}, \tag{19}$$

then $\mathcal{H}(\mathbf{k})$ at $k_y=0,\pi$ becomes off-diagonal,

$$\mathcal{H}(\mathbf{k}) = \begin{pmatrix} 0 & q(\mathbf{k}) \\ q^\dagger(\mathbf{k}) & 0 \end{pmatrix}. \tag{20}$$

By using $q(\mathbf{k})$ in the above, the topological number $I(k_y)$ is defined as

$$I(k_y) = \frac{1}{4\pi i}\int_{-\pi}^{\pi} dk_x\, \mathrm{tr}[q^{-1}(\mathbf{k})\partial_{k_x}q(\mathbf{k}) - q^{\dagger-1}(\mathbf{k})\partial_{k_x}q^\dagger(\mathbf{k})]. \tag{21}$$

We call $I(k_y)$ as the winding number in the following.

As is shown in Appendix B 3, the winding number and the TKNN number satisfies

$$(-1)^{I_{\mathrm{TKNN}}} = (-1)^{I(0)-I(\pi)}. \tag{22}$$

Therefore, from the winding number, we can determine $(-1)^{I_{\mathrm{TKNN}}}$. The index $(-1)^{I_{\mathrm{TKNN}}}$ is of particular interest since it give a hallmark of the non-Abelian topological phase: when $(-1)^{I_{\mathrm{TKNN}}}=-1$, there are an odd number of Majorana zero modes in a vortex, which implies the vortex is a non-Abelian anyon. In the following sections, we calculate the winding number and the TKNN number for the cases of the *s*-wave pairing state and the $d+id$ pairing state. The obtained phase diagrams for the non-Abelian topological phases are summarized in Fig. 1.

A. *s*-wave pairing

We consider an *s*-wave NCS superconductor with the gap function

$$\Delta(\mathbf{k}) = \Delta_s. \tag{23}$$

For the s-wave NCS superconductor, $q(\mathbf{k})$ is given by

$$q(\mathbf{k}) = -[\varepsilon(\mathbf{k}) - \mu_B H_z \sigma_z - \alpha \sin k_x \sigma_y] + i\Delta_s \sigma_y, \tag{24}$$

thus its determinant is

$$\det q(\mathbf{k}) = \varepsilon(\mathbf{k})^2 - (\mu_B H_z)^2 - \alpha^2 \sin^2 k_x + \Delta_s^2 - 2i\alpha\Delta_s \sin k_x. \tag{25}$$

Denoting the real (imaginary) part of $\det q(\mathbf{k})$ as $m_1(\mathbf{k})$ $(m_2(\mathbf{k}))$, we have

$$m_1(\mathbf{k}) = \varepsilon(\mathbf{k})^2 - (\mu_B H_z)^2 - \alpha^2 \sin^2 k_x + \Delta_s^2,$$
$$m_2(\mathbf{k}) = -2\alpha\Delta_s \sin k_x. \tag{26}$$

From formula (B22) in Appendix B 2, the winding number is evaluated as

$$I(k_y) = \frac{1}{2}\{-\mathrm{sgn}[\varepsilon(0,k_y)^2 - (\mu_B H_z)^2 + \Delta_s^2] + \mathrm{sgn}[\varepsilon(\pi,k_y)^2 - (\mu_B H_z)^2 + \Delta_s^2]\}. \tag{27}$$

In Table I, we summarize the winding number $I(k_y)$ calculated from this equation. We also list $(-1)^{I_{\mathrm{TKNN}}}$ obtained from formula (22). Note that the topological numbers can change only when one of the gap closing conditions [Eq. (8)] is met. From Table I, we obtain the diagram of the non-Abelian topological phase for s-wave pairing shown in Fig. 1(a).

To get a better understanding of the origin of the non-Abelian topological order, we, here, present some physical discussions about the phase diagram shown in Fig. 1(a). We consider two different but complementary arguments. The first one is based on mapping from the s-wave pairing state to an effective spinless p-wave pairing state in the chirality basis. The second one is the argument based on the duality relation introduced in Sec. IV. The former is applicable to the case of $\mu_B H_z \gg \Delta_s$ while the latter is particularly useful in the vicinity of the topological phase-transition point $\mu_B H_z \sim \Delta_s$. In this sense, these two arguments are complementary.

We, first, present the former argument which utilizes the mapping onto an effective p-wave pairing state in the chirality basis representation and is applicable to the case of $\mu_B H_z \gg \Delta_s$. In the chirality basis, the SO coupling term and the Zeeman coupling one in the Hamiltonian are diagonalized, leading to the two SO split bands. As is shown in Appendix C, in the parameter region where the non-Abelian topological phase is realized, we can map our model (4) into a spinless chiral p-wave superconductor in the chirality basis, provided that $\mu_B H_z \gg \Delta_s$. For $\mu < 0$, the low-energy effective Hamiltonian in this case is

$$\tilde{\mathcal{H}}_-(\mathbf{k}) = \begin{pmatrix} \varepsilon(\mathbf{k}) - \Delta\varepsilon(\mathbf{k}) & [\alpha\mathcal{L}_{0x}(\mathbf{k}) - i\alpha\mathcal{L}_{0y}(\mathbf{k})][\Delta(\mathbf{k})/\Delta\varepsilon(\mathbf{k})] \\ [\alpha\mathcal{L}_{0x}(\mathbf{k}) + i\alpha\mathcal{L}_{0y}(\mathbf{k})][\Delta^*(\mathbf{k})/\Delta\varepsilon(\mathbf{k})] & -\varepsilon(\mathbf{k}) + \Delta\varepsilon(\mathbf{k}) \end{pmatrix} \tag{28}$$

and for $\mu > 0$, it is

$$\tilde{\mathcal{H}}_+(\mathbf{k}) = \begin{pmatrix} \varepsilon(\mathbf{k}) + \Delta\varepsilon(\mathbf{k}) & [\alpha\mathcal{L}_{0x}(\mathbf{k}) + i\alpha\mathcal{L}_{0y}(\mathbf{k})][\Delta(\mathbf{k})/\Delta\varepsilon(\mathbf{k})] \\ [\alpha\mathcal{L}_{0x}(\mathbf{k}) - i\alpha\mathcal{L}_{0y}(\mathbf{k})][\Delta^*(\mathbf{k})/\Delta\varepsilon(\mathbf{k})] & -\varepsilon(\mathbf{k}) - \Delta\varepsilon(\mathbf{k}) \end{pmatrix} \tag{29}$$

with $\Delta\varepsilon(\mathbf{k}) = \sqrt{[\alpha\mathcal{L}_0(\mathbf{k})]^2 + (\mu_B H_z)^2}$. For the s-wave pairing state in the original Hamiltonian, the gap function in Eq. (28) or Eq. (29) is given by

$$[\alpha\mathcal{L}_{0x}(\mathbf{k}) \mp i\alpha\mathcal{L}_{0y}(\mathbf{k})][\Delta(\mathbf{k})/\Delta\varepsilon(\mathbf{k})] \sim i\alpha(\sin k_x \mp i \sin k_y)(\Delta_s/\mu_B H_z), \tag{30}$$

thus, for both μ's, the chiral $p+ip$ wave superconductors are realized in the chirality basis. By using the effective Hamiltonian, the phase diagram of our system can be understood more intuitively. The above effective Hamiltonian (28) or Eq. (29) is obtained by using the fact that, when $\mu_B H_z \gg \Delta_s$, and μ is in the region of the phase diagram where the non-Abelian topological order is realized, only one of the two Fermi surfaces survives and the other is pushed away by the Zeeman magnetic field. As a result, the spinless chiral $p+ip$-wave superconductor is realized effectively. The non-Abelian topological phase obtained here is effectively the same as that in the spinless chiral $p+ip$-wave superconductor.

We, now, present the second argument on the origin of the topological order which is based on the duality relation.[37] To grasp the physics shown in the phase diagram, let us see what happens at the transition between the trivial phase (i.e., the phase with $\mu_B H_z = 0$) and the non-Abelian topological one $[(-1)^{I_{\mathrm{TKNN}}} = -1]$. From Fig. 1(a), it is found that if we increase the Zeeman magnetic field, such a phase transition occurs at $\mu = \pm 4t$ when $\mu_B H_z = \Delta_s$. For simplicity, we consider the case with $\mu = -4t$, where the Fermi surface is close to the Γ point. A similar analysis is possible for the transition at $\mu = 4t$. In the former case, the gap of the system closes at $\mathbf{k} = (0,0)$.

To examine the topological phase transition, it is convenient to use the dual Hamiltonian instead of the original one. Using the duality transformation [Eq. (11)], we recast the original BdG Hamiltonian into its unitary equivalent dual Hamiltonian $\mathcal{H}_D(\mathbf{k})$. Then, we find that for $\mu \sim -4t$, the dual

TABLE I. The TKNN integer I_{TKNN} and the winding number $I(k_y)$ for 2D s-wave superconductors with the Rashba coupling. $(-1)^{I_{\mathrm{TKNN}}}=-1$ corresponds to the non-Abelian topological phase.

(a) $\mu \le -2t$

$(\mu_B H_z)^2$	$(-1)^{I_{\mathrm{TKNN}}}$	$I(0)$	$I(\pi)$
$0<(\mu_B H_z)^2<(4t+\mu)^2+\Delta_s^2$	1	0	0
$(4t+\mu)^2+\Delta_s^2<(\mu_B H_z)^2<\mu^2+\Delta_s^2$	−1	1	0
$\mu^2+\Delta_s^2<(\mu_B H_z)^2<(4t-\mu)^2+\Delta_s^2$	−1	0	1
$(4t-\mu)^2+\Delta_s^2<(\mu_B H_z)^2$	1	0	0

(b) $-2t<\mu\le 0$

$(\mu_B H_z)^2$	$(-1)^{I_{\mathrm{TKNN}}}$	$I(0)$	$I(\pi)$
$0<(\mu_B H_z)^2<\mu^2+\Delta_s^2$	1	0	0
$\mu^2+\Delta_s^2<(\mu_B H_z)^2<(4t+\mu)^2+\Delta_s^2$	1	−1	1
$(4t+\mu)^2+\Delta_s^2<(\mu_B H_z)^2<(4t-\mu)^2+\Delta_s^2$	−1	0	1
$(4t-\mu)^2+\Delta_s^2<(\mu_B H_z)^2$	1	0	0

(c) $0<\mu\le 2t$

$(\mu_B H_z)^2$	$(-1)^{I_{\mathrm{TKNN}}}$	$I(0)$	$I(\pi)$
$0<(\mu_B H_z)^2<\mu^2+\Delta_s^2$	1	0	0
$\mu^2+\Delta_s^2<(\mu_B H_z)^2<(4t-\mu)^2+\Delta_s^2$	1	−1	1
$(4t-\mu)^2+\Delta_s^2<(\mu_B H_z)^2<(4t+\mu)^2+\Delta_s^2$	−1	−1	0
$(4t+\mu)^2+\Delta_s^2<(\mu_B H_z)^2$	1	0	0

(d) $2t<\mu$

$(\mu_B H_z)^2$	$(-1)^{I_{\mathrm{TKNN}}}$	$I(0)$	$I(\pi)$
$0<(\mu_B H_z)^2<(4t-\mu)^2+\Delta_s^2$	1	0	0
$(4t-\mu)^2+\Delta_s^2<(\mu_B H_z)^2<\mu^2+\Delta_s^2$	−1	0	−1
$\mu^2+\Delta_s^2<(\mu_B H_z)^2<(4t+\mu)^2+\Delta_s^2$	−1	−1	0
$(4t+\mu)^2+\Delta_s^2<(\mu_B H_z)^2$	1	0	0

Hamiltonian $\mathcal{H}_{\mathrm{D}}(\mathbf{k})$ around $\mathbf{k}=(0,0)$ is decomposed into the following two 2×2 matrices,

$$\mathcal{H}^D_{\uparrow\uparrow}(\mathbf{k})=\begin{pmatrix}\Delta_s-\mu_B H_z & \alpha(k_y+ik_x)\\ \alpha(k_y-ik_x) & -\Delta_s+\mu_B H_z\end{pmatrix}, \tag{31}$$

$$\mathcal{H}^D_{\downarrow\downarrow}(\mathbf{k})=\begin{pmatrix}\Delta_s+\mu_B H_z & \alpha(-k_y+ik_x)\\ \alpha(-k_y-ik_x) & -\Delta_s-\mu_B H_z\end{pmatrix}, \tag{32}$$

where $\uparrow$ and $\downarrow$ denote the spin in the basis of the dual Hamiltonian.

We notice here that these Hamiltonians have a close similarity to the Hamiltonian of the spinless chiral $p+ip$ superconductor discussed in Ref. 5. The spinless chiral $p+ip$-wave superconductor shows a phase transition between the non-Abelian topological phase (or weak-pairing phase in the terminology used in Ref. 5) and the topologically trivial phase (strong-pairing phase), and the transition is described by the following low-energy effective Hamiltonian:

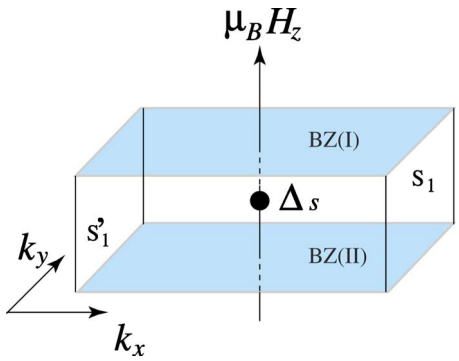

FIG. 2. (Color online) Topological phase transition at $\mu_B H_z=\Delta_s$. BZ(I) and BZ(II) indicate the Brillouin zones after and before the transition, respectively. The gap closes at $(k_x,k_y)=(0,0)$ when $\mu_B H_z=\Delta_s$. S_i and S_i' $(i=1,2)$ are the side faces of the rectangle in which the top and bottom faces are BZ(I) and BZ(II). For simplicity, only S_1 and S_1' are explicitly indicated.

$$\mathcal{H}_{p+ip}(\mathbf{k})=\begin{pmatrix}\mu_p & \Delta_p(k_x+ik_y)\\ \Delta_p^*(k_x-ik_y) & -\mu_p\end{pmatrix}, \tag{33}$$

where μ_p and Δ_p are the chemical potential and the paring amplitude for the $p+ip$-wave superconductor, respectively. For $\mu_p>0$, the state is topologically trivial, and for $\mu_p<0$, the state supports non-Abelian topological order. The phase transition occurs at $\mu_p=0$. By identifying $\Delta_s-\mu_B H_z$ and α in Eq. (31) with μ_p and Δ_p in Eq. (33), respectively, the similarity between $\mathcal{H}_{\uparrow\uparrow}(\mathbf{k})$ and $\mathcal{H}_{p+ip}(\mathbf{k})$ is evident. This similarity immediately implies that the phase transition at $\mu_B H_z=\Delta_s$ is also accompanied with the emergence of the non-Abelian topological order. (We also have a similar phase transition at $\mu_B H_z=-\Delta_s$ by decreasing the Zeeman magnetic field. From the similarity between $\mathcal{H}^D_{\downarrow\downarrow}(\mathbf{k})$ and $\mathcal{H}_{p+ip}(\mathbf{k})$, this transition is also found to be accompanied with the emergence of the non-Abelian topological order.)

Indeed, using the dual Hamiltonian (31), we can see directly that the TKNN number change by $\Delta I_{\mathrm{TKNN}}=-1$ at the transition. For this purpose, we slightly generalize the gauge field $A_i^{(-)}(\mathbf{k})$ as follows:

$$A_\mu^{(-)}(\mathbf{k})=\begin{cases} i\sum_{E_n<0}\langle\phi_n(\mathbf{k})|\partial_{k_\mu}\phi_n(\mathbf{k})\rangle & \text{for } \mu=x,y,\\ i\sum_{E_n<0}\langle\phi_n(\mathbf{k})|\partial_{\mu_B H_z}\phi_n(\mathbf{k})\rangle & \text{for } \mu=z,\end{cases} \tag{34}$$

where the z component is introduced additionally. Then, consider the rectangle illustrated in Fig. 2. Here the top face BZ(I) and the bottom one BZ(II) denote the first Brillouin zones of the system after $(\mu_B H_z>\Delta_s)$ and before $(\mu_B H_z<\Delta_s)$ the transition, respectively. Because of the periodicity of the Block wave function $|\phi_n(\mathbf{k})\rangle$ in the momentum space, "the magnetic field" $\mathcal{F}_\mu^{(-)}(\mathbf{k})=\epsilon_{\mu\nu\lambda}\partial_{k_\nu}A_\lambda^{(-)}(\mathbf{k})$ on the side faces S_i $(i=1,2)$ are identical to that on the opposite ones S_i'. Therefore, the change in the TKNN number

$$\Delta I_{\mathrm{TKNN}} = \frac{1}{2\pi}\int_{\mathrm{BZ(I)}} dk_x dk_y \mathcal{F}^{(-)}(\mathbf{k}) - \frac{1}{2\pi}\int_{\mathrm{BZ(II)}} dk_x dk_y \mathcal{F}^{(-)}(\mathbf{k}) \tag{35}$$

is rewritten as the total magnetic field penetrating the surface of the rectangle ∂V,

$$\begin{aligned}\Delta I_{\mathrm{TKNN}} &= \frac{1}{2\pi}\int_{\mathrm{BZ(I)}} dk_x dk_y \mathcal{F}_z^{(-)}(\mathbf{k}) - \frac{1}{2\pi}\int_{\mathrm{BZ(II)}} dk_x dk_y \mathcal{F}_z^{(-)}(\mathbf{k}) \\ &+ \frac{1}{2\pi}\int_{\mathrm{S}_1} dk_y dk_z \mathcal{F}_x^{(-)}(\mathbf{k}) - \frac{1}{2\pi}\int_{\mathrm{S}_1'} dk_y dk_z \mathcal{F}_x^{(-)}(\mathbf{k}) \\ &+ \frac{1}{2\pi}\int_{\mathrm{S}_2} dk_z dk_x \mathcal{F}_y^{(-)}(\mathbf{k}) - \frac{1}{2\pi}\int_{\mathrm{S}_2'} dk_z dk_x \mathcal{F}_y^{(-)}(\mathbf{k}) \\ &= \frac{1}{2\pi}\int_{\partial V} dS_\mu \mathcal{F}_\mu^{(-)}(\mathbf{k}),\end{aligned} \tag{36}$$

with $k_z = \mu_{\mathrm{B}} H_z - \Delta_s$. Therefore, ΔI_{TKNN} is nonzero only if the "magnetic monopole" of $A_\mu^{(-)}(\mathbf{k})$ exists inside the rectangle: if there is no such a source of the magnetic field, ΔI_{TKNN} should be zero from the Gauss-Bonnet theorem. On the other hand, if the magnetic monopole exists, we have a net magnetic flux penetrating the surface of the rectangle.

Actually, we have a magnetic monopole located at $(k_x, k_y, k_z(=\mu_{\mathrm{B}} H_z - \Delta_s)) = (0,0,0)$, where the gap of the system closes. The magnetic charge can be read from the dual Hamiltonian $\mathcal{H}_{\uparrow\uparrow}^{\mathrm{D}}(\mathbf{k})$. By rewriting $\mathcal{H}_{\uparrow\uparrow}^{\mathrm{D}}(\mathbf{k})$ as $\mathcal{H}_{\uparrow\uparrow}^{\mathrm{D}}(\mathbf{k}) = \mathbf{R}(\mathbf{k}) \cdot \boldsymbol{\sigma}$ with $(R_1(\mathbf{k}), R_2(\mathbf{k}), R_3(\mathbf{k})) = (\alpha k_y, -\alpha k_x, -k_z)$, the monopole charge is given by

$$\mathcal{Q} = \frac{1}{8\pi}\int_{S^2} dS_\lambda \epsilon_{\lambda\mu\nu} \hat{\mathbf{R}} \cdot (\partial_{k_\mu} \hat{\mathbf{R}} \times \partial_{k_\nu} \hat{\mathbf{R}}), \tag{37}$$

where $\hat{\mathbf{R}}(\mathbf{k}) = \mathbf{R}(\mathbf{k})/|\mathbf{R}(\mathbf{k})|$ and S^2 a small sphere surrounding the gap-closing point. Noting that the right-hand side of Eq. (37) counts the number of times the unit vector $\hat{\mathbf{R}}$ wraps around the origin, we obtain $\mathcal{Q} = -1$. Therefore, from Eq. (36), we immediately find that $\Delta I_{\mathrm{TKNN}} = -1$. Before the transition, the system is topologically equivalent to the ordinary s-wave superconductor without the Zeeman magnetic field, thus $I_{\mathrm{TKNN}} = 0$. Therefore, we have $I_{\mathrm{TKNN}} = -1$ after the transition.[38] Again, this result indicates that the system after the transition belongs to the same topological class as the spinless chiral $p+ip$-wave superconductor with $I_{\mathrm{TKNN}} = -1$.

As mentioned before, the above two arguments are applicable, respectively, to the different parameter regions, and thus, they are complementary. It is noted that these arguments are also straightforwardly applied to the case of the $d+id$ pairing state discussed in the next sections.

As seen from Table I, the non-Abelian topological order [i.e., $(-1)^{I_{\mathrm{TKNN}}} = -1$] appears only in the case that the Zeeman energy $\mu_{\mathrm{B}} H_z$ is larger than the superconducting gap Δ_s. As is well known, the Rashba superconductors are stable against the Pauli depairing effect due to applied magnetic fields even for $\mu_{\mathrm{B}} H_z > \Delta_s$ when the magnetic field is applied perpendicular to the xy plane,[33,35] as long as the Rashba SO interaction is sufficiently strong. However, there is also the orbital depairing effect due to applied magnetic field. An important question is how the superconductivity survives the orbital depairing effect for such a strong magnetic field $\mu_{\mathrm{B}} H_z > \Delta_s$. One possible scenario is to realize this system in the proximity between a superconductor and a semiconductor as proposed in Refs. 27 and 28. Another possibility is to realize it in strongly correlated electron systems for which the orbital depairing field is large. Also, one more promising scheme is to utilize ultracold fermionic atom as proposed in Ref. 26. This issue will be discussed in more detail in Sec. IX.

B. $d+id$ wave pairing

1. Case of $\Delta(\mathbf{k}) = \Delta_d^{(1)}(\cos k_y - \cos k_x) + i\Delta_d^{(2)} \sin k_x \sin k_y$

For the case of the $d+id$-wave superconductor with the gap function

$$\Delta(\mathbf{k}) = \Delta_d^{(1)}(\cos k_y - \cos k_x) + i\Delta_d^{(2)} \sin k_x \sin k_y, \tag{38}$$

$q(\mathbf{k})$ and its determinant are given by

$$\begin{aligned} q(\mathbf{k}) &= -[\varepsilon(\mathbf{k}) - \mu_{\mathrm{B}} H_z \sigma_z - \alpha \sin k_x \sigma_y] \\ &+ i\Delta_d^{(1)}(\cos k_y - \cos k_x)\sigma_y, \end{aligned} \tag{39}$$

$$\begin{aligned} \det q(\mathbf{k}) &= \varepsilon(\mathbf{k})^2 - (\mu_{\mathrm{B}} H_z)^2 - \alpha^2 \sin^2 k_x \\ &+ [\Delta_d^{(1)}(\cos k_y - \cos k_x)]^2 \\ &- 2i\alpha \sin k_x \Delta_d^{(1)}(\cos k_y - \cos k_x). \end{aligned} \tag{40}$$

Therefore, the real and imaginary parts of the determinants are

$$\begin{aligned} m_1(\mathbf{k}) &= \varepsilon(\mathbf{k})^2 - (\mu_{\mathrm{B}} H_z)^2 - \alpha^2 \sin^2 k_x \\ &+ [\Delta_d^{(1)}(\cos k_y - \cos k_x)]^2, \end{aligned} \tag{41}$$

$$m_2(\mathbf{k}) = -2i\alpha \sin k_x \Delta_d^{(1)}(\cos k_y - \cos k_x).$$

To apply formula (B22), we slightly change $m_2(\mathbf{k})$ as $-2i\alpha \sin k_x \Delta_d^{(1)}(\cos k_y - \cos k_x) + \delta$ ($\delta \ll 1$). After using formula (B22), we put $\delta = 0$ again. Since $I(k_y)$ is a topological number, this procedure does not change the value of $I(k_y)$. In this manner, we estimate the winding number $I(k_y)$ as

$$\begin{aligned} I(0) = \frac{1}{2}\{&-\mathrm{sgn}[\varepsilon(0,0)^2 - (\mu_{\mathrm{B}} H_z)^2] + \mathrm{sgn}[\varepsilon(\pi,0)^2 - (\mu_{\mathrm{B}} H_z)^2 \\ &+ 4(\Delta_d^{(1)})^2]\} \end{aligned} \tag{42}$$

and

$$\begin{aligned} I(\pi) = \frac{1}{2}\{&-\mathrm{sgn}[\varepsilon(\pi,\pi)^2 - (\mu_{\mathrm{B}} H_z)^2] + \mathrm{sgn}[\varepsilon(0,\pi)^2 - (\mu_{\mathrm{B}} H_z)^2 \\ &+ 4(\Delta_d^{(1)})^2]\}. \end{aligned} \tag{43}$$

We summarize the winding number $I(k_y)$ and $(-1)^{I_{\mathrm{TKNN}}}$ in Table II. The non-Abelian phases are realized in the parameter regions that $(-1)^{I_{\mathrm{TKNN}}} = -1$. From Table II, we obtain the phase diagram shown in Fig. 1(b).

In a manner similar to the NCS s-wave superconductor, if $\mu_{\mathrm{B}} H_z \gg \Delta(\mathbf{k})$, the obtained phase diagram can be understood

TABLE II. The TKNN integer I_{TKNN} and the winding number $I(k_y)$ for the 2D $d+id$-wave NCS superconductor with $\Delta(\mathbf{k})=\Delta_d^{(1)}(\cos k_y-\cos k_x)+i\Delta_d^{(2)}\sin k_x \sin k_y$. $(-1)^{I_{\mathrm{TKNN}}}=-1$ corresponds to the non-Abelian topological phase.

(a) $\mu \le -2t+(\Delta_d^{(1)})^2/2t$

$(\mu_B H_z)^2$	$(-1)^{I_{\mathrm{TKNN}}}$	$I(0)$	$I(\pi)$
$0<(\mu_B H_z)^2<(4t+\mu)^2$	1	0	0
$(4t+\mu)^2<(\mu_B H_z)^2<\mu^2+4(\Delta_d^{(1)})^2$	−1	1	0
$\mu^2+4(\Delta_d^{(1)})^2<(\mu_B H_z)^2<(4t-\mu)^2$	−1	0	−1
$(4t-\mu)^2<(\mu_B H_z)^2$	1	0	0

(b) $-2t+(\Delta_d^{(1)})^2/2t<\mu\le 0$

$(\mu_B H_z)^2$	$(-1)^{I_{\mathrm{TKNN}}}$	$I(0)$	$I(\pi)$
$0<(\mu_B H_z)^2<\mu^2+4(\Delta_d^{(1)})^2$	1	0	0
$\mu^2+4(\Delta_d^{(1)})^2<(\mu_B H_z)^2<(4t+\mu)^2$	1	−1	−1
$(4t+\mu)^2<(\mu_B H_z)^2<(4t-\mu)^2$	−1	0	−1
$(4t-\mu)^2<(\mu_B H_z)^2$	1	0	0

(c) $0<\mu\le 2t-(\Delta_d^{(1)})^2/2t$

$(\mu_B H_z)^2$	$(-1)^{I_{\mathrm{TKNN}}}$	$I(0)$	$I(\pi)$
$0<(\mu_B H_z)^2<\mu^2+4(\Delta_d^{(1)})^2$	1	0	0
$\mu^2+4(\Delta_d^{(1)})^2<(\mu_B H_z)^2<(4t-\mu)^2$	1	−1	−1
$(4t-\mu)^2<(\mu_B H_z)^2<(4t+\mu)^2$	−1	−1	0
$(4t+\mu)^2<(\mu_B H_z)^2$	1	0	0

(d) $2t-(\Delta_d^{(1)})^2/2t<\mu$

$(\mu_B H_z)^2$	$(-1)^{I_{\mathrm{TKNN}}}$	$I(0)$	$I(\pi)$
$0<(\mu_B H_z)^2<(4t-\mu)^2$	1	0	0
$(4t-\mu)^2<(\mu_B H_z)^2<\mu^2+4(\Delta_d^{(1)})^2$	−1	0	1
$\mu^2+4(\Delta_d^{(1)})^2<(\mu_B H_z)^2<(4t+\mu)^2$	−1	−1	0
$(4t+\mu)^2<(\mu_B H_z)^2$	1	0	0

by the effective Hamiltonian (28) for $\mu<0$ or Eq. (29) for $\mu>0$ obtained in the chirality basis. For simplicity, suppose that $\Delta_d^{(1)}=\Delta_d^{(2)}\equiv\Delta_d$. The gap function in Eq. (28) or Eq. (29) yields

$$[\alpha\mathcal{L}_{0x}(\mathbf{k})\pm i\alpha\mathcal{L}_{0y}(\mathbf{k})][\Delta(\mathbf{k})/\Delta\varepsilon(\mathbf{k})] \sim \mp i\alpha(\sin k_x \pm i \sin k_y)(\cos k_y-\cos k_x+i\sin k_x \sin k_y)\times(\Delta_d/\mu_B H_z), \quad (44)$$

thus the chiral $f+if$-wave superconductor or the chiral $p+ip$-wave superconductor is realized both in the effective Hamiltonians $\tilde{\mathcal{H}}_{\mp}(\mathbf{k})$. [Whether the p-wave state or the f-wave state realizes depends on the relative chirality between the $d+id$ order parameter and the p-wave factor in Eq. (44) which stems from the SO interaction.] Therefore, the non-Abelian topological phases obtained here are effectively the same as that in either the spinless chiral $f+if$-wave superconductor or the spinless chiral $p+ip$-wave superconductor.

One remarkable point observed from Table II [or Fig. 1(b)] is that, in contrast to the s-wave pairing case, for the $d+id$-wave pairing state, the non-Abelian topological order appears even for small but nonzero magnetic fields, provided that $\mu\sim\pm 4t$. Thus, in this case, we do not need to worry about the orbital depairing effect due to applied magnetic fields. This point makes it easier to realize the Majorana fermion state in the $d+id$ Rashba superconductor than in the s-wave pairing state from the perspective of the stability against applied magnetic fields, though, unfortunately, the experimental realization of $d+id$ superconductors has not yet been established to this date.

Since the $d+id$ pairing state breaks time-reversal symmetry, the TKNN number is nonzero even for zero magnetic fields. In the absence of the Zeeman field, we can evaluate the TKNN number I_{TKNN} directly. In this case, we smoothly eliminate the Rashba SO interaction by setting $\alpha\to 0$ without gap closing. This means that the TKNN number of the $d+id$-wave NCS superconductor is the same as that of the $d+id$ superconductor without the Rashba coupling.

2. Case of $\Delta(\mathbf{k})=\Delta_d^{(1)}(\sin^2 k_x-\sin^2 k_y)+i\Delta_d^{(2)}\sin k_x \sin k_y$

For the $d+id$-wave NCS superconductor with the gap function

$$\Delta(\mathbf{k})=\Delta_d^{(1)}(\sin^2 k_x-\sin^2 k_y)+i\Delta_d^{(2)}\sin k_x \sin k_y, \quad (45)$$

$q(\mathbf{k})$ is given by

$$q(\mathbf{k})=-[\varepsilon(\mathbf{k})-\mu_B H_z\sigma_z-\alpha \sin k_x\sigma_y]+i\Delta_d^{(1)}\sin^2 k_x\sigma_y. \quad (46)$$

Thus its determinant becomes

$$\det q(\mathbf{k})=\varepsilon(\mathbf{k})^2-(\mu_B H_z)^2-\alpha^2\sin^2 k_x+(\Delta_d^{(2)})^2\sin^4 k_x - 2i\alpha\Delta_d^{(1)}\sin^3 k_x, \quad (47)$$

and the real and imaginary parts of the determinant are

$$m_1(\mathbf{k})=\varepsilon(\mathbf{k})^2-(\mu_B H_z)^2-\alpha^2\sin^2 k_x + (\Delta_d^{(1)})^2\sin^4 k_x, \quad m_2(\mathbf{k})=-2\alpha\Delta_d^{(1)}\sin^3 k_x. \quad (48)$$

In a manner similar to the previous d-wave case, we regulate $m_2(\mathbf{k})$ as $m_2(\mathbf{k})\to -2\alpha\Delta_d^{(1)}\sin^3 k_x+\delta^3$ $(\delta\ll 1)$. Then, we obtain

$$I(k_y)=\frac{1}{2}\{-\mathrm{sgn}[\varepsilon(0,k_y)^2-(\mu_B H_z)^2]+\mathrm{sgn}[\varepsilon(\pi,k_y)^2-(\mu_B H_z)^2]\}. \quad (49)$$

We summarize the winding number $I(k_y)$ and $(-1)^{I_{\mathrm{TKNN}}}$ in Table III. The results are also summarized in the phase diagram, Fig. 1(c).

When $\mu_B H_z \gg \Delta(\mathbf{k})$, the obtained non-Abelian topological phase can be understood by using the effective Hamiltonian (28) or Eq. (29) in a manner similar to the previous cases. In the parameter region where the non-Abelian topological phase is realized, only one of the Fermi surfaces survives and the other is pushed away by the Zeeman magnetic field, then,

TABLE III. The TKNN integer I_{TKNN} and the winding number $I(k_y)$ for the 2D $d+id$-wave NCS superconductor with $\Delta(\mathbf{k})=\Delta_d^{(1)}(\sin^2 k_x-\sin^2 k_y)+i\Delta_d^{(2)}\sin k_x \sin k_y$. $(-1)^{I_{\mathrm{TKNN}}}=-1$ corresponds to the non-Abelian topological phase.

(a) $\mu \le -2t$

$(\mu_B H_z)^2$	$(-1)^{I_{\mathrm{TKNN}}}$	$I(0)$	$I(\pi)$
$0<(\mu_B H_z)^2<(4t+\mu)^2$	1	0	0
$(4t+\mu)^2<(\mu_B H_z)^2<\mu^2$	−1	1	0
$\mu^2<(\mu_B H_z)^2<(4t-\mu)^2$	−1	0	1
$(4t-\mu)^2<(\mu_B H_z)^2$	1	0	0

(b) $-2t<\mu\le 0$

$(\mu_B H_z)^2$	$(-1)^{I_{\mathrm{TKNN}}}$	$I(0)$	$I(\pi)$
$0<(\mu_B H_z)^2<\mu^2$	1	0	0
$\mu^2<(\mu_B H_z)^2<(4t+\mu)^2$	1	−1	1
$(4t+\mu)^2<(\mu_B H_z)^2<(4t-\mu)^2$	−1	0	1
$(4t-\mu)^2<(\mu_B H_z)^2$	1	0	0

(c) $0<\mu\le 2t$

$(\mu_B H_z)^2$	$(-1)^{I_{\mathrm{TKNN}}}$	$I(0)$	$I(\pi)$
$0<(\mu_B H_z)^2<\mu^2$	1	0	0
$\mu^2<(\mu_B H_z)^2<(4t-\mu)^2$	1	−1	1
$(4t-\mu)^2<(\mu_B H_z)^2<(4t+\mu)^2$	−1	−1	0
$(4t+\mu)^2<(\mu_B H_z)^2$	1	0	0

(d) $2t<\mu$

$(\mu_B H_z)^2$	$(-1)^{I_{\mathrm{TKNN}}}$	$I(0)$	$I(\pi)$
$0<(\mu_B H_z)^2<(4t-\mu)^2$	1	0	0
$(4t-\mu)^2<(\mu_B H_z)^2<\mu^2$	−1	0	−1
$\mu^2<(\mu_B H_z)^2<(4t+\mu)^2$	−1	−1	0
$(4t+\mu)^2<(\mu_B H_z)^2$	1	0	0

it is found that the non-Abelian topological phases obtained here are effectively the same as that in either the spinless chiral $f+if$-wave superconductor or the spinless chiral $p+ip$-wave superconductor.

As in the previous section, the non-Abelian topological order is realized even for small but nonzero magnetic fields, provided that $\mu \sim \pm 4t$. This is a generic feature of the $d+id$-wave pairing state. However, in contrast to the case of $\Delta(\mathbf{k})=\Delta_d^{(1)}(\cos k_y-\cos k_x)+i\Delta_d^{(2)}\sin k_x \sin k_y$, the parameters which distinguish different phases do not depend on the superconducting gap function.

VI. MAJORANA CHIRAL EDGE STATE

In this section, we investigate edge states for the 2D spin-singlet NCS superconductors numerically. From the bulk-edge correspondence, a nontrivial bulk topological number implies the existence of gapless edge states. In the case of TRB superconductors, the gapless edge states are a chiral Majorana fermion mode. We confirm this in the following.

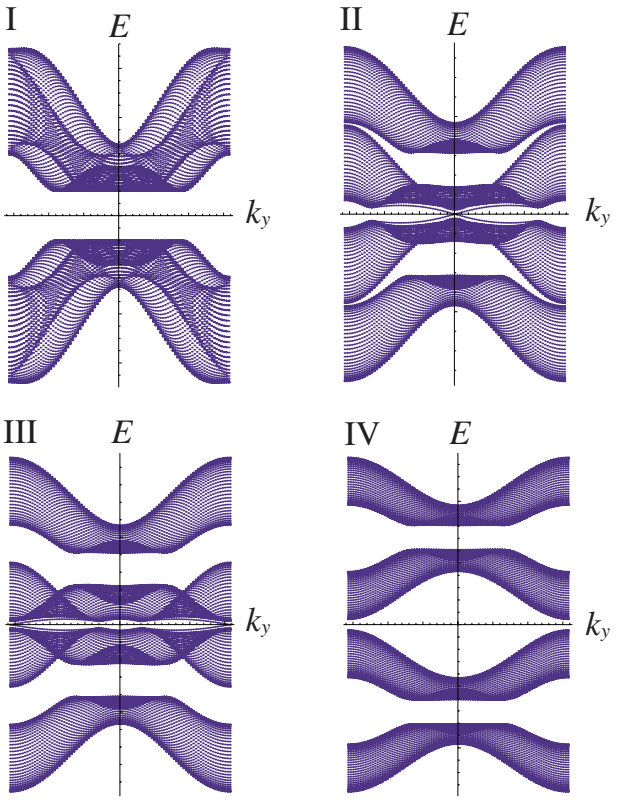

FIG. 3. (Color online) The energy spectra of the 2D s-wave NCS superconductor with open edges at $i_x=0$ and $i_x=30$ for $\mu<-2t$. Here k_y denotes the momentum in the y direction, and $k_y \in [-\pi,\pi]$. We take $t=1$, $\mu=-2.5$, $\lambda=0.5$, and $\Delta_s=1$. The Zeeman magnetic field H_z is (I) $\mu_B H_z=0$, (II) $\mu_B H_z=2$, (III) $\mu_B H_z=3$, and (IV) $\mu_B H_z=7$. The cases of (I)–(IV) correspond to, respectively, the four regions in Table I, (a). The non-Abelian phases are (II) and (III). The two gapless modes found in (II) correspond to edge modes for two open edges, respectively. Thus, they are chiral. The same is also true for the gapless modes in (III).

A. s wave

To study edge states, we consider the lattice version of Hamiltonian (1). For an s-wave NCS superconductor, the lattice Hamiltonian is given by

$$\mathcal{H}=\mathcal{H}_{\mathrm{kin}}+\mathcal{H}_{\mathrm{SO}}+\mathcal{H}_s, \tag{50}$$

$$\mathcal{H}_{\mathrm{kin}}=-t\sum_{\langle \mathbf{i},\mathbf{j}\rangle,\sigma} c_{\mathbf{i}\sigma}^\dagger c_{\mathbf{j}\sigma}-\mu\sum_{\mathbf{i},\sigma} c_{\mathbf{i}\sigma}^\dagger c_{\mathbf{i}\sigma}-\mu_B H_z\sum_{\mathbf{i},\sigma,\sigma'}(\sigma_z)_{\sigma\sigma'} c_{\mathbf{i}\sigma}^\dagger c_{\mathbf{i}\sigma'}, \tag{51}$$

$$\mathcal{H}_{\mathrm{SO}}=-\lambda\sum_{\mathbf{i}}[(c_{\mathbf{i}-\hat{x}\downarrow}^\dagger c_{\mathbf{i}\uparrow}-c_{\mathbf{i}+\hat{x}\downarrow}^\dagger c_{\mathbf{i}\uparrow}) + i(c_{\mathbf{i}-\hat{y}\downarrow}^\dagger c_{\mathbf{i}\uparrow}-c_{\mathbf{i}+\hat{y}\downarrow}^\dagger c_{\mathbf{i}\uparrow})+\mathrm{H.c.}], \tag{52}$$

$$\mathcal{H}_s=\Delta_s(c_{\mathbf{i}\uparrow}^\dagger c_{\mathbf{i}\downarrow}^\dagger+\mathrm{H.c.}), \tag{53}$$

where $\mathbf{i}=(i_x,i_y)$ denotes a site on the square lattice, $c_{\mathbf{i}\sigma}^\dagger$ ($c_{\mathbf{i}\sigma}$) the creation (annihilation) operator of an electron with spin σ at site $\mathbf{i}$, and $\lambda=\alpha/2$. The sum $\Sigma_{\langle \mathbf{i},\mathbf{j}\rangle}$ is taken between the

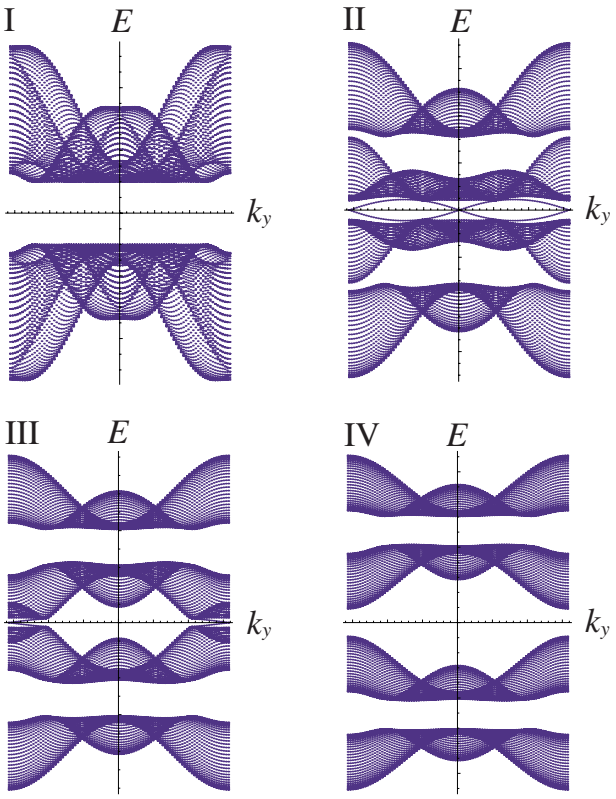

FIG. 4. (Color online) The energy spectra of the 2D s-wave NCS superconductor with open edges at $i_x=0$ and $i_x=30$ for $-2t<\mu<0$. Here k_y denotes the momentum in the y direction, and $k_y \in [-\pi,\pi]$. We take $t=1$, $\mu=-1$, $\lambda=0.5$, and $\Delta_s=1$. The Zeeman magnetic field H_z is (I) $\mu_B H_z=0$, (II) $\mu_B H_z=2$, (III) $\mu_B H_z=4$, and (IV) $\mu_B H_z=6$. The cases of (I)–(IV) correspond to, respectively, the four regions in Table I, (b). The non-Abelian phase is (III).

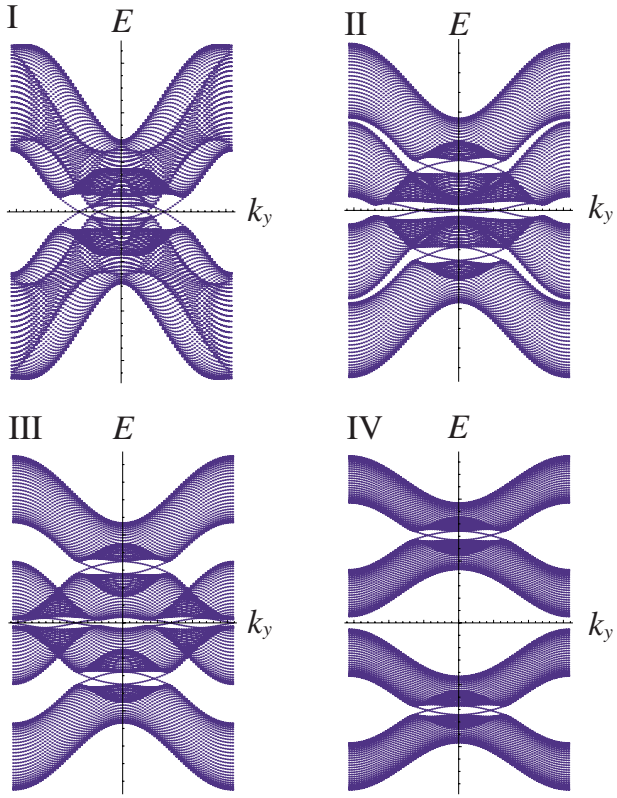

FIG. 5. (Color online) The energy spectra of the 2D $d+id$-wave NCS superconductor $[\Delta(\mathbf{k})=\Delta_d^{(1)}(\cos k_y-\cos k_x)+i\Delta_d^{(2)}\sin k_x \sin k_y]$ with open edges at $i_x=0$ and $i_x=30$ for $\mu<-2t+(\Delta_d^{(1)})^2/2t$. Here k_y denotes the momentum in the y direction and $k_y \in [-\pi,\pi]$. We take $t=1$, $\mu=-2.5$, $\lambda=0.5$, $\Delta_d^{(1)}=0.5$, and $\Delta_d^{(2)}=0.8$. The Zeeman magnetic field H_z is (I) $\mu_B H_z=0$, (II) $\mu_B H_z=2$, (III) $\mu_B H_z=3$, and (IV) $\mu_B H_z=7$. The cases of (I)–(IV) correspond to, respectively, the four regions in Table II, (a). The non-Abelian phases are (II) and (III).

nearest-neighbor sites. Suppose that the system has two open boundary edges at $i_x=0$ and $i_x=N_x$, and impose the periodic boundary condition in the y direction. By solving numerically the energy spectrum as a function of the momentum k_y in the y direction, we study edge states.

We illustrate the energy spectra for the 2D s-wave NCS superconductor with edges at $i_x=0$ and $i_x=30$ in Figs. 3 and 4. In Fig. 3 (Fig. 4), μ satisfies $\mu<-2t$ $(-2t<\mu<0)$, and the corresponding bulk topological numbers are given in Table I, (a) [Table I, (b)]. We find that if the TKNN number is odd, odd numbers of gapless edge modes appear. In this case, the non-Abelian topological order appears, and the edge zero mode is a chiral Majorana fermion. It is also found that when the winding number $I(k_y)$ is nonzero for $k_y=0$, or π, the energy of the gapless edge mode becomes zero at this value of k_y. Therefore, all the results are consistent with the existence of the correspondence between the bulk topological numbers and the edge spectra.

B. $d+id$ wave

1. Case of $\Delta(\mathbf{k})=\Delta_d^{(1)}(\cos k_y-\cos k_x)+i\Delta_d^{(2)}\sin k_x \sin k_y$

The lattice Hamiltonian for the 2D $d+id$-wave NCS superconductor with $\Delta(\mathbf{k})=\Delta_d^{(1)}(\cos k_y-\cos k_x)+i\Delta_d^{(2)}\sin k_x \sin k_y$ is given by $\mathcal{H}=\mathcal{H}_{\rm kin}+\mathcal{H}_{\rm SO}+\mathcal{H}_s$ with

$$\mathcal{H}_s=-\frac{\Delta_d^{(1)}}{4}[c^\dagger_{\mathbf{i}+\hat{x}\uparrow}c^\dagger_{\mathbf{i}\downarrow}+c^\dagger_{\mathbf{i}-\hat{x}\uparrow}c^\dagger_{\mathbf{i}\downarrow}-c^\dagger_{\mathbf{i}+\hat{y}\uparrow}c^\dagger_{\mathbf{i}\downarrow}-c^\dagger_{\mathbf{i}-\hat{y}\uparrow}c^\dagger_{\mathbf{i}\downarrow}]$$
$$-i\frac{\Delta_d^{(2)}}{4}[c^\dagger_{\mathbf{i}+\hat{x}+\hat{y}\uparrow}c^\dagger_{\mathbf{i}\downarrow}+c^\dagger_{\mathbf{i}-\hat{x}-\hat{y}\uparrow}c^\dagger_{\mathbf{i}\downarrow}-c^\dagger_{\mathbf{i}+\hat{x}-\hat{y}\uparrow}c^\dagger_{\mathbf{i}\downarrow}-c^\dagger_{\mathbf{i}-\hat{x}+\hat{y}\uparrow}c^\dagger_{\mathbf{i}\downarrow}]$$
$$+\text{H.c.} \tag{54}$$

The kinetic term $\mathcal{H}_{\rm kin}$ and the Rashba SO interaction $\mathcal{H}_{\rm SO}$ are the same as Eqs. (51) and (52), respectively.

In a manner similar to the s-wave NCS superconductor, we obtain the energy spectra for the system with edges at $i_x=0$ and $i_x=30$ numerically. We illustrate the energy spectra for the 2D d-wave NCS superconductor with the gap function $\Delta(\mathbf{k})=\Delta_d^{(1)}(\cos k_y-\cos k_x)+i\Delta_d^{(2)}\sin k_x \sin k_y$ in Figs. 5 and 6. In Fig. 5 (Fig. 6), μ satisfies $\mu<-2t+(\Delta_d^{(1)})^2/2t(-2t+(\Delta_d^{(1)})^2/2t<\mu<0)$, and the corresponding bulk topological numbers are given in Table II, (a) [Table II, (b)]. We find that if the TKNN number is odd, odd numbers of gapless edge

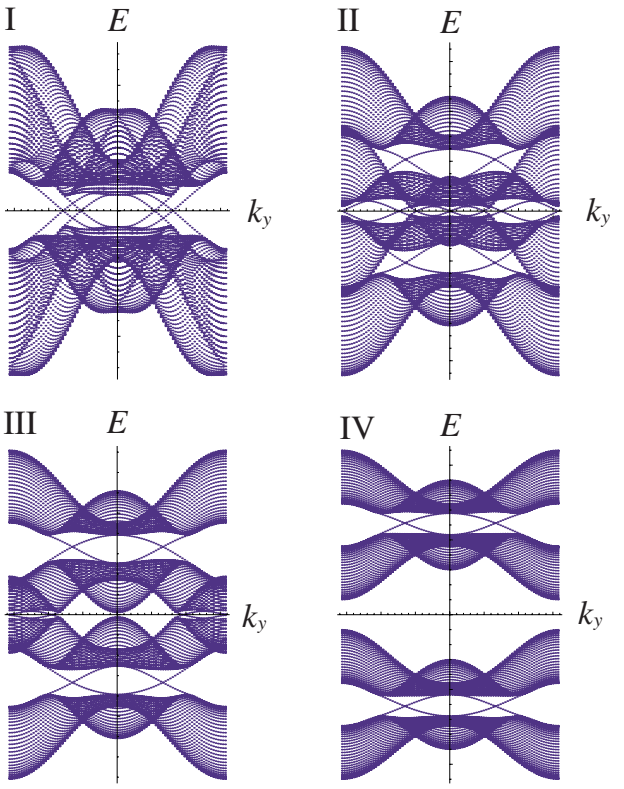

FIG. 6. (Color online) The energy spectra of the 2D $d+id$-wave NCS superconductor $[\Delta(\mathbf{k})=\Delta_d^{(1)}(\cos k_y-\cos k_x)+i\Delta_d^{(2)}\sin k_x \sin k_y]$ with open edges at $i_x=0$ and $i_x=30$ for $-2t+(\Delta_d^{(1)})^2/2t<\mu<0$. Here k_y denotes the momentum in the y direction and $k_y\in[-\pi,\pi]$. We take $t=1$, $\mu=-1$, $\lambda=0.5$, $\Delta_d^{(1)}=0.5$, and $\Delta_d^{(2)}=0.8$. The Zeeman magnetic field H_z is (I) $\mu_B H_z=0$, (II) $\mu_B H_z=1.6$, (III) $\mu_B H_z=3.1$, and (IV) $\mu_B H_z=6$. The cases of (I)–(IV) correspond to, respectively, the four regions in Table II, (b). The non-Abelian phase is (III).

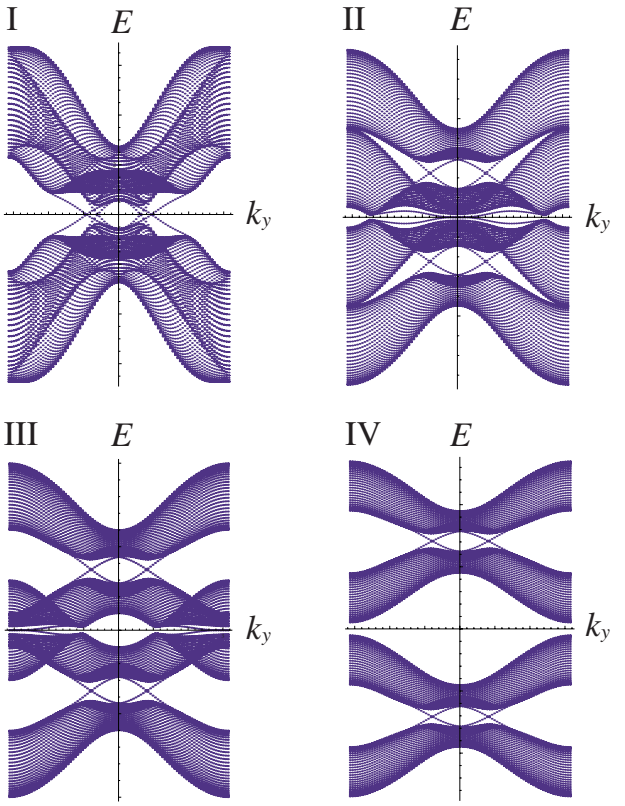

FIG. 7. (Color online) The energy spectra of the 2D $d+id$-wave NCS superconductor $[\Delta(\mathbf{k})=\Delta_d^{(1)}(\sin^2 k_x-\sin^2 k_y)+i\Delta_d^{(2)}\sin k_x \sin k_y]$ with open edges at $i_x=0$ and $i_x=30$ for $\mu<-2t$. Here k_y denotes the momentum in the y direction and $k_y\in[-\pi,\pi]$. We take $t=1$, $\mu=-2.5$, $\lambda=0.5$, $\Delta_d^{(1)}=1$, and $\Delta_d^{(2)}=1$. The Zeeman magnetic field H_z is (I) $\mu_B H_z=0$, (II) $\mu_B H_z=2$, (III) $\mu_B H_z=3.5$, and (IV) $\mu_B H_z=7$. The cases of (I)–(IV) correspond to, respectively, the four regions in Table III, (a). The non-Abelian phases are (II) and (III).

modes appear. The non-Abelian topological order (and hence the chiral Majorana fermion mode) is realized in this case. In addition, it is found that if the winding number $I(k_y)$ ($k_y=0,\pi$) is nonzero for some k_y, the energy of the gapless edge state becomes zero at this value of k_y. These results are consistent with the bulk-edge correspondence.

Since the $d+id$-wave superconductor breaks time-reversal symmetry even in the absence of a magnetic field, the TKNN number is nonzero for $H_z=0$, and there are four chiral edge modes, which are seen in diagram (I) in Figs. 5–8. Since there are even numbers of gapless edge modes, they do not behave as non-Abelian anyons. These edge modes crosses the zero energy at some $k_y\neq 0,\pm\pi$. In contrast, the Majorana fermion mode associated with the non-Abelian topological order crosses the zero energy at $k_y=0$ or π corresponding to the nonzero values of the winding number $I(k_y)$ at these points.

2. *Case of* $\Delta(\mathbf{k})=\Delta_d^{(1)}(\sin^2 k_x-\sin^2 k_y)+i\Delta_d^{(2)}\sin k_x \sin k_y$

In this case, we use the lattice Hamiltonian $\mathcal{H}=\mathcal{H}_{\rm kin}+\mathcal{H}_{\rm SO}+\mathcal{H}_s$ with

$$\mathcal{H}_s=-\frac{\Delta_d^{(1)}}{4}[c^\dagger_{\mathbf{i}+2\hat{x}\uparrow}c^\dagger_{\mathbf{i}\downarrow}+c^\dagger_{\mathbf{i}-2\hat{x}\uparrow}c^\dagger_{\mathbf{i}\downarrow}-c^\dagger_{\mathbf{i}+2\hat{y}\uparrow}c^\dagger_{\mathbf{i}\downarrow}-c^\dagger_{\mathbf{i}-2\hat{y}\uparrow}c^\dagger_{\mathbf{i}\downarrow}]$$
$$-i\frac{\Delta_d^{(2)}}{4}[c^\dagger_{\mathbf{i}+\hat{x}+\hat{y}\uparrow}c^\dagger_{\mathbf{i}\downarrow}+c^\dagger_{\mathbf{i}-\hat{x}-\hat{y}\uparrow}c^\dagger_{\mathbf{i}\downarrow}-c^\dagger_{\mathbf{i}+\hat{x}-\hat{y}\uparrow}c^\dagger_{\mathbf{i}\downarrow}-c^\dagger_{\mathbf{i}-\hat{x}+\hat{y}\uparrow}c^\dagger_{\mathbf{i}\downarrow}]$$
$$+\text{H.c.} \tag{55}$$

Here, the kinetic term $\mathcal{H}_{\rm kin}$ and the Rashba SO interaction $\mathcal{H}_{\rm SO}$ are the same as Eqs. (51) and (52), respectively.

We calculate the energy spectra for the system with edges at $i_x=0$ and $i_x=30$ numerically. The energy spectra for the 2D d-wave NCS superconductor with the gap function $\Delta(\mathbf{k})=\Delta_d^{(1)}(\sin^2 k_x-\sin^2 k_y)+i\Delta_d^{(2)}\sin k_x \sin k_y$ are shown in Figs. 7 and 8. In Fig. 7 (Fig. 8), μ satisfies $\mu<-2t$ ($-2t<\mu<0$), and the corresponding bulk topological numbers are given in Table III, (a) [Table III, (b)]. When the TKNN number is odd, odd numbers of gapless edge states appear, signifying the non-Abelian topological order. It is also found that if the winding number $I(k_y)$ ($k_y=0,\pi$) is nonzero for

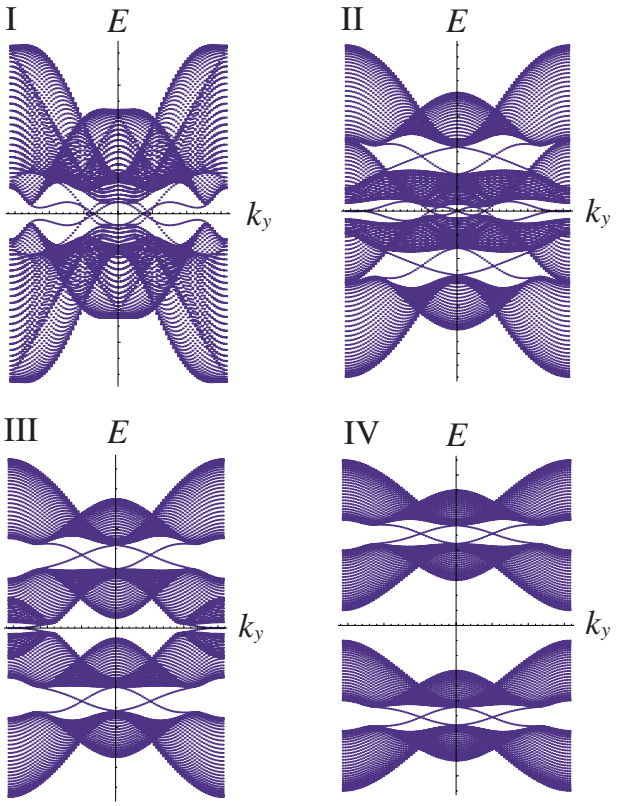

FIG. 8. (Color online) The energy spectra of the 2D $d+id$-wave NCS superconductor $[\Delta(\mathbf{k})=\Delta_d^{(1)}(\sin^2 k_x-\sin^2 k_y)+i\Delta_d^{(2)}\sin k_x \sin k_y]$ with open edges at $i_x=0$ and $i_x=30$ for $-2t<\mu<0$. Here k_y denotes the momentum in the y direction and $k_y \in [-\pi,\pi]$. We take $t=1$, $\mu=-1$, $\lambda=0.5$, $\Delta_d^{(1)}=1$, and $\Delta_d^{(2)}=1$. The Zeeman magnetic field H_z is (I) $\mu_B H_z=0$, (II) $\mu_B H_z=2$, (III) $\mu_B H_z=3.5$, and (IV) $\mu_B H_z=6$. The cases of (I)–(IV) correspond to, respectively, the four regions in Table III, (b). The non-Abelian phase is (III).

some k_y, the energy of the gapless edge state becomes zero at this value of k_y. These results are consistent with the bulk-edge correspondence again.

VII. MAJORANA ZERO MODE IN A VORTEX OF AN s-WAVE RASHBA SUPERCONDUCTOR

In this section, we discuss a Majorana fermion mode in a vortex core of an s-wave Rashba superconductor, which is one of the important features of the non-Abelian topological order, and relevant to the application to the topological quantum computation. We also discuss that, in certain parameter region, the Majorana mode in the s-wave Rashba superconductors is strongly stable against thermal noise and intervortex tunneling, which are serious obstructions to the implementation of the topological quantum computation in the case of $p+ip$ superconductors.

A. Majorana solution of the Bogoliubov-de Gennes equation

The non-Abelian topological order is characterized by the existence of the Majorana zero-energy mode in a vortex core, which leads to the realization of the non-Abelian statistics. In this section, we demonstrate that the Majorana fermion mode in a vortex core exists for an s-wave Rashba superconductor when the Zeeman energy $\mu_B H_z$ is larger than the superconducting gap $\Delta=\Delta_s$, by solving the BdG equation for a single vortex of the superconducting order parameter; $\Delta(\mathbf{r})=\Delta\exp(in\theta)$ with n vorticity. In Ref. 26, when n is odd, the Majorana bound state for a vortex of the SO interaction is obtained by the analysis of the BdG equation for the dual Hamiltonian (11). The existence of the Majorana bound state in a vortex of the SO interaction strongly implies that there exists the Majorana bound state also in a vortex of the superconducting condensate because these two vortex states are related by a singular gauge transformation. In the following, we will find the zero-energy Majorana solution for a vortex core of the superconducting condensate explicitly in the case that the vorticity n is odd, and the condition $\mu_B H_z>\Delta>0$ is satisfied. This result is in accordance with the finding of Sau *et al.*[27] In the following analysis, instead of using the dual Hamiltonian (11), we deal with the BdG equation for the original Hamiltonian (4) directly. Since we cannot obtain the exact solution of the BdG equation analytically, we adopt the following approximation scheme. As clarified in the previous sections, the non-Abelian topological order appears when the Fermi level crosses $\mathbf{k}$ points in the vicinity of the Γ point or the M point in the Brillouin zone. In this situation, there are two Fermi surfaces split by the Rashba SO interaction. One is located in the vicinity of the Γ (or M) point with the Fermi momentum $\mathbf{k}_F\sim 0$ [or (π,π)], and the other has the large Fermi momentum $\mathbf{k}_F \neq 0,(\pi,\pi)$. Since the momentum is not a good quantum number in the presence of a vortex core, a bound state in the vortex core generally consists of a superposition of quasiparticles from both of these two Fermi surfaces. However, according to the discussion based on the duality Hamiltonian given in Sec. V A, it is strongly suggested that in the vicinity of the topological phase-transition point $\mu_B H_z\sim\Delta$, quasiparticles with $\mathbf{k}\sim 0$ [or (π,π)] play a very important role in the realization of the non-Abelian topological order. This implies that when the Zeeman energy is close to the superconducting gap, the Majorana fermion mode is mainly formed by quasiparticles with $\mathbf{k}_F\sim 0$ or (π,π) rather than those with $\mathbf{k}_F \neq 0,(\pi,\pi)$, in the long-distance asymptotic regime away from the center of the vortex core. Thus, in the following, we try to construct an approximate solution for the zero-energy mode in a vortex from quasiparticles with $\mathbf{k}_F\sim 0$ or (π,π). As will be shown below, the vortex core for this approximated solution has a characteristic length $\sim v_F/(\mu_B H_z-\Delta)$ while quasiparticles with $\mathbf{k}_F\neq 0,(\pi,\pi)$ give contributions to the vortex core bound state with a characteristic length $\sim v_F/\Delta$. Thus, the approximated solution presented in the following is valid when $0<\mu_B H_z-\Delta<\Delta$ in the long-distance asymptotic regime.

To solve the BdG equation, we choose the gauge for which the gap function is real by applying the gauge transformation $e\mathbf{A}\to e\mathbf{A}-n\nabla\theta/2$, $\Delta\exp(in\theta)\to\Delta$. Then, the BdG equation is

$$\mathcal{H}\tilde{\Psi}=E\tilde{\Psi}, \tag{56}$$

$$\mathcal{H} = \begin{pmatrix} \varepsilon\left(\hat{\mathbf{k}} - e\mathbf{A} + \frac{n}{2}\nabla\theta\right) + \mathbf{g}\left(\hat{\mathbf{k}} - e\mathbf{A} + \frac{n}{2}\nabla\theta\right)\cdot\boldsymbol{\sigma} - h\sigma_z & \Delta i\sigma_y \\ -\Delta i\sigma_y & -\varepsilon\left(\hat{\mathbf{k}} + e\mathbf{A} - \frac{n}{2}\nabla\theta\right) + \mathbf{g}\left(\hat{\mathbf{k}} + e\mathbf{A} - \frac{n}{2}\nabla\theta\right)\cdot\boldsymbol{\sigma}^* + h\sigma_z \end{pmatrix}. \quad (57)$$

Here $\tilde{\Psi}^T = (\tilde{u}_\uparrow, \tilde{u}_\downarrow, \tilde{v}_\uparrow, \tilde{v}_\downarrow)$, $\varepsilon(\mathbf{k}) = \frac{\mathbf{k}^2}{2m} - \mu_0$, $\mathbf{g}(\mathbf{k}) = 2\lambda(k_y, -k_x, 0)$, $\hat{\mathbf{k}} = -i\nabla$, and $h = \mu_B H_z$. Assuming $H_z \ll H_{c2}$, we neglect $e\mathbf{A}$ compared to $n\nabla\theta/2$ in $\varepsilon(\hat{\mathbf{k}} - e\mathbf{A} + \frac{n}{2}\nabla\theta)$ and $\mathbf{g}(\hat{\mathbf{k}} - e\mathbf{A} + \frac{n}{2}\nabla\theta)$.[39] We also assume that $\Delta = 0$ for $r < r_c$, and $\Delta \neq 0$ for $r > r_c$, where $r_c \ll \xi$. For simplicity, we consider the case of $\mu_0 = 0$, for which one of the two SO split bands crosses the Γ point $\mathbf{k} = 0$. This is a typical situation which realizes the non-Abelian topological order (and hence the Majorana zero mode) as discussed in the previous sections. In the following, we restrict our analysis to the zero-energy state with $E = 0$. Furthermore, we impose the condition that the magnitude of the SO interaction is much larger than the Zeeman energy scale; i.e., $h \ll m\lambda^2$. Under this condition, we can find the following approximated solution for the zero-energy mode in a vortex core with the odd vorticity n. For $r < r_c$,

$$\tilde{u}_\uparrow(r,\theta) = A_\uparrow e^{-i(\theta/2)} H^{(1)}_{(n-1/2)}\left(i\frac{hr}{2\lambda}\right), \quad (58)$$

$$\tilde{u}_\downarrow(r,\theta) = -iA_\uparrow e^{i(\theta/2)} H^{(1)}_{(n+1/2)}\left(i\frac{hr}{2\lambda}\right), \quad (59)$$

and for $r > r_c$,

$$\tilde{u}_\uparrow(r,\theta) = \sqrt{2}A_\uparrow e^{-i(\theta/2)} e^{\int^r dr'(h-\Delta)/2\lambda} H^{(1)}_{(n+3/2)}\left(i\frac{h-\Delta}{\lambda}r\right), \quad (60)$$

$$\tilde{u}_\downarrow(r,\theta) = -i\sqrt{2}A_\uparrow e^{i(\theta/2)} e^{\int^r dr'(h-\Delta)/2\lambda} H^{(1)}_{(n+1/2)}\left(i\frac{h-\Delta}{\lambda}r\right), \quad (61)$$

where $H^{(1)}_\nu(z)$ is the first Hankel function and the constant $A_\uparrow$ is determined by the normalization condition. Also, $\tilde{v}_\sigma(r,\theta) = \tilde{u}_\sigma(r,\theta)$. The solution for $r > r_c$ and those for $r < r_c$ can be matched at $r = r_c$ by using the asymptotic form of the Hankel function, as explained in Appendix D. Since there is only one zero-energy mode, the above solution indicates that there is a Majorana zero-energy mode in a vortex core with odd vorticity. Note that this approximated solution is constructed from quasiparticles in the vicinity of the Γ point $\mathbf{k} \sim 0$. As seen from Eqs. (60) and (61), the above solution for the vortex core bound state decays as $\sim\exp(-\frac{h-\Delta}{2\lambda}r)$ in the long-distance regime. On the other hand, the contribution from quasiparticles with the large Fermi momentum to the vortex core state decays like $\sim\exp(-\frac{\Delta}{2\lambda}r)$ (note that when $\mu_0 = 0$, the Fermi velocity $v_F \sim 2\lambda$). Thus, for $0 < h - \Delta < \Delta$, the long-distance behavior of the vortex core state is dominated by quasiparticles with $\mathbf{k} \sim 0$, and hence the above approximated solution mainly constructed from quasiparticles with $\mathbf{k} \sim 0$ is valid under this condition.

In the above derivation of the zero-energy Majorana bound state, we have used several approximations. In particular, at the stage of matching the solutions for $r > r_c$ and $r < r_c$, we have neglected corrections of order $O[h/(m\lambda^2)]$. Actually, such approximations are not essential for the realization of the Majorana zero-energy mode, but, rather, required by our approximation method of the construction of the zero mode. In fact, the exact solution for the zero-energy mode in a vortex core should be a superposition of quasiparticles with $\mathbf{k} \sim 0$ and those with $k_F \neq 0$ because the momentum is not a good quantum number in the presence of a vortex core. Since it is quite difficult to obtain the exact solution of the zero-energy mode constructed from both quasiparticles with $\mathbf{k} \sim 0$ and those with $k_F \neq 0$, we approximate it by the bound state mainly formed by quasiparticles with $\mathbf{k} \sim 0$, neglecting contributions of quasiparticles from the large Fermi surface. Because of this approximation, we need the additional approximations mentioned above, when we match the solutions for $r > r_c$ and $r < r_c$. We expect that for the exact solution of the zero-energy Majorana mode, the weight of quasiparticles from the large Fermi surface may become substantially large in the short-distance region in the vicinity of the center of the vortex core, compared to the contributions from quasiparticles with $\mathbf{k} \sim 0$. If we properly include the mixing with quasiparticles from the large Fermi surface, we may be able to match the solutions without such additional approximations. Also, our zero-energy solution is not regular at $r = 0$, though it is still normalizable, and physically allowed. We expect that this singular behavior for $r \sim 0$ is also raised by our approximation neglecting the mixing with quasiparticles from the large Fermi surface, which should be important for small r. If one takes into account contributions of quasiparticles from the large Fermi surface, it may be possible to cure this singular behavior of our solution at $r = 0$. Nevertheless, when the conditions $h \ll m\lambda^2$ and $0 < h - \Delta < \Delta$ is satisfied, the zero-energy solution may be dominated by quasiparticles with $\mathbf{k} \sim 0$ in the long-distance asymptotic regime sufficiently far away from the center of the vortex core, and our analytical solution obtained above may become a good approximation.

We would like to note that although the zero-energy solution given by Eqs. (60) and (61) with the asymptotic forms of Eqs. (D29) and (D30) in Appendix D looks like localized even in the limit of $\Delta \to 0$, this never means that there is a zero-energy Majorana bound state in the normal state. In fact, the above zero-energy solution is not applicable to the

normal state without a vortex because of the following reason. The zero-energy solutions in the normal state are indeed given by Eqs. (58) and (59). However, the Hankel function is not regular at $r=0$. This singularity is unphysical because in the absence of a vortex in the normal state, translation invariance is recovered, and thus, there should not be a special point in the coordinate space at which the wave function is singular. This implies that the zero-energy solution given by Eqs. (58) and (59) is not allowed in the normal state without a vortex. Thus, there is no zero-energy bound state in the limit of $\Delta \to 0$. The Majorana bound state in a vortex core exists only for $\mu_B H_z > \Delta > 0$.

The above analysis may be also extended to the case of $d+id$-wave pairing straightforwardly, since the $d+id$-wave state, which is the superposition of the $d_{x^2-y^2}$-wave state and the d_{xy}-wave state, is an eigenstate of the orbital angular momentum operator, as in the case of the s-wave pairing, and the treatment for the gap function given above is applicable. We obtain the Majorana fermion mode for a nonzero magnetic field $h>0$ in the case of the $d+id$-wave pairing, which is consistent with the existence of the chiral Majorana edge discussed in Sec. VI.

We stress again that the Majorana zero-energy mode in a vortex core is formed mainly by the superposition of an electron and a hole with the vanishing Fermi momentum $k_F \sim 0$ in the long-distance asymptotic regime, provided that the energy scale of the SO interaction is sufficiently larger than the Zeeman energy and that $0 < h - \Delta < \Delta$. As will be discussed in the following, this property is very important for the stability of the Majorana fermion against various sources of decoherence which exist in real materials and may destroy the Majorana fermion acting as a qubit.

B. Strong stability of the Majorana fermion mode against thermal noise

For the detection of the non-Abelian anyons and also for the implementation of the topological quantum computation utilizing them, it is desirable that the Majorana zero-energy state in a vortex core is well separated from excited states, the interaction with which may cause decoherence. As was pointed out in Ref. 26, in the non-Abelian phase of s-wave Rashba superconductors, when the energy scale of the SO interaction is much larger than the Zeeman energy and the condition $0 < \mu_B H_z - \Delta < \Delta$ is satisfied, the excitation energy of the vortex core state is of order $\mu_B H_z - \Delta$, which is much larger than the typical size of the excitation energy in the vortex core bound state of weak-coupling superconductors, i.e., $\sim \Delta^2 / E_F$.[39] Thus, the Majorana fermion mode found here is quite stable against thermal noise even at moderately low temperatures, to which it is not difficult to access within standard experimental techniques. We, here, explain the origin of the strong stability of the Majorana mode in more details. The excitation energy in the vortex core is due to the kinetic energy of quasiparticles in the Andreev bound state, which stems from the derivative term in Eqs. (D1) and (D2) in Appendix D. We restrict the following argument within the case that the magnitude of the SO interaction is much larger than the Zeeman energy, and that the condition $0 < \mu_B H_z - \Delta < \Delta$ is satisfied. In this case, the Majorana solution is constructed mainly from quasiparticles with $\mathbf{k} \sim 0$, as clarified in the previous section. Then, the first-order derivative terms $2\lambda(\frac{\partial}{\partial r} \pm \frac{i}{r}\frac{\partial}{\partial \theta})$ give leading contributions to the kinetic energy. On the other hand, from the solution of the BdG equation [Eqs. (60) and (61)], we see that the characteristic size of the vortex core is $\xi_{\rm core} \sim 2\lambda/(\mu_B H_z - \Delta)$. Thus, the excitation energy is of the order $\sim 2\lambda/[2\lambda/(\mu_B H_z - \Delta)] \sim \mu_B H_z - \Delta$. This large magnitude of the excitation energy implies that the Majorana zero-energy mode in the s-wave Rashba superconductor with $\mu_B H_z > \Delta$ is significantly stable against thermal noise, compared to chiral $p+ip$ superconductors. Also, such large excitation energy ensures that the experimental detection of the non-Abelian anyons is quite feasible for our system. The origin of the strong stability of the Majorana fermion mode is deeply related to the fact that it is mainly constructed from quasiparticles in the Dirac cone at the Γ point in the Brillouin zone for $0 < \mu_B H_z - \Delta < \Delta$ in the long-distance asymptotic regime, as mentioned above. Since the Dirac cone has a vanishing Fermi momentum, the kinetic energy is dominated by the SO interaction which is of order $\lambda/\xi_{\rm core}$ rather than the standard kinetic-energy term of order $\xi_{\rm core}^{-2}/(2m)$. This feature leads to the strong stability of the Majorana zero-energy mode. It is noted that the robustness of the Majorana fermion mode in the s-wave Rashba superconductor was also pointed out in Ref. 40 from a different point of view.

C. Stability against decoherence due to intervortex tunneling

It has been proposed that the Majorana fermion modes in superconductors can be utilized as decoherence-free qubits, which enable us the construction of the fault-tolerant topological quantum computer.[12–14,41] Two Majorana fermions, say γ_1 and γ_2, constitute one complex fermion state described by $\psi = \gamma_1 + i\gamma_2$, which is occupied or unoccupied.

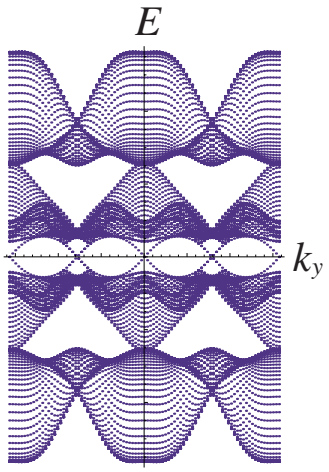

FIG. 9. (Color online) The energy spectra of the NCS SDW state with edges at $i_x=0$ and $i_x=30$. Here k_y denotes the momentum in the y direction and $k_y \in [-\pi, \pi]$. We take $t=1=\alpha=1=\Delta_S=1$. The Zeeman magnetic field H_z is $\mu_B H_z=1.5$. At $k_y=0, \pm\pi/2, \pi$, we have gapless states on each edge. These gapless edge modes are chiral.

This doubly degenerate state stores a qubit nonlocally, which is protected against any local perturbations, as long as the distance between two vortices, each of which contains one Majorana mode is sufficiently large. One crucial obstruction to this scheme is the decoherence raised by intervortex tunneling; tunneling processes between two Majorana modes in two vortices lift the degeneracy, leading to decoherence. In particular, it was pointed out by Cheng *et al.*[29] that the energy of the complex fermion ψ exhibits quantum oscillation as a function of the spatial separation r between two vortices as $\sim\cos k_F r$ with k_F the Fermi momentum, and thus takes both positive and negative values depending on r. This rapid change in the sign of the energy seriously flaws the initialization and the readout of the qubit.

Here, we discuss the drastic suppression of the quantum oscillation for intervortex tunneling in the Rashba s-wave superconductors in a particular parameter region. As explained in Sec. VII A, the zero-energy Majorana bound state in a vortex core obtained above consists of two contributions; one from quasiparticles with $\mathbf{k}\sim 0$ and the other from quasiparticles with the large k_F. The former contribution has the characteristic length scale of order $\lambda/(\mu_B H_z-\Delta)$, as clarified by the solution [Eqs. (60) and (61)]. On the other hand, for the latter contribution, the characteristic length scale is of order λ/Δ since the Fermi velocity is of order λ when $\mu_0 \sim 0$ in Eq. (57). Then, in the case of $0<\mu_B H_z-\Delta<\Delta$, the Majorana zero mode is mainly formed by quasiparticles with the vanishing Fermi momentum $k_F\sim 0$ in the long-distance asymptotic regime. That is, in the tunneling process between two vortices separated by the distance R, the overlap of the component with $\mathbf{k}\sim 0$, which is of order $\exp[-R(\mu_B H_z -\Delta)/\lambda]$ is much larger in the magnitude than the oscillating contribution from the large Fermi surface which is of order $\exp(-R\Delta/\lambda)\cos(k_F R)$ for large R. The intervortex tunneling mediated via quasiparticles with $k_F\sim 0$ does not involve the quantum oscillation, making a sharp contrast to Majorana modes found in $p+ip$ superconductors. As a result, the energy of a complex fermion made of the two Majorana fermions is dominated by the nonoscillating part from quasiparticles with $\mathbf{k}\sim 0$, and thus, the decoherence due to the quantum oscillation is suppressed. It is noted that this protection mechanism also works for a Majorana fermion mode in the proximity between a topological insulator and an s-wave superconductor,[23] as long as the chemical potential is properly tuned to realize $k_F\sim 0$ for the surface Dirac cone. Since momentum is not conserved in the vicinity of a vortex, there may be hybridization between the Majorana state in a vortex core and quasiparticles with the finite Fermi momentum, which raises intervortex tunneling involving the quantum oscillation. However, the analysis of the zero-energy Majorana mode in a vortex core in the previous sections implies that we can construct the zero-energy Majorana state which is mainly formed by quasiparticles with $\mathbf{k}\sim 0$, provided that the energy scale of the SO interaction is much larger than the Zeeman energy, and that $0<\mu_B H_z-\Delta<\Delta$. Thus, it may be possible to realize the Majorana fermion in the vortex core of the Rashba superconductor which is stable against decoherence due to the intervortex tunneling.

VIII. TOPOLOGICAL DENSITY WAVE STATES AND CHARGE FRACTIONALIZATION

The above argument for the non-Abelian topological order in s-wave superconductors implies that topological order is realizable in conventional spin (or charge)-density wave states. The Hamiltonian for the s-wave superconductivity on a bipartite lattice is mapped to the Hamiltonian for the SDW state or the CDW state by changing the basis of fermion fields. Thus, an s-wave superconducting state with the topological order can be mapped to a density wave state with a certain topological order. As shown below, the topological order in the density wave state is Abelian, and quasiparticles in this topological order are not Majorana fermions, but possess $U(1)$ charge. However, the quasiparticles exhibit charge fractionalization which characterizes the Abelian topological order.

A. Topological spin-density wave state

We, first, consider the SDW state with the order parameter $\Delta_S=\langle c^\dagger_{\mathbf{k}\uparrow} c_{\mathbf{k}+\mathbf{Q}\uparrow}\rangle=-\langle c^\dagger_{\mathbf{k}\downarrow} c_{\mathbf{k}+\mathbf{Q}\downarrow}\rangle$, where $\mathbf{Q}$ is the ordering wave number vector. We also assume that there are the Rashba-type SO interaction and the Zeeman magnetic field $h=\mu_B H_z$. Then, the mean-field Hamiltonian is given by

$$\mathcal{H}_{\mathrm{SDW}}=\frac{1}{2}\sum_{\mathbf{k}}\Psi^\dagger_{\mathbf{k}}\mathcal{H}_{\mathrm{SDW}}(\mathbf{k})\Psi_{\mathbf{k}} \tag{62}$$

with

$$\mathcal{H}_{\mathrm{SDW}}(\mathbf{k})=\begin{pmatrix}\varepsilon(\mathbf{k})-h\sigma_z+\alpha\mathcal{L}_0(\mathbf{k})\cdot\boldsymbol{\sigma} & i\Delta_S\sigma_y \\ -i\Delta_S\sigma_y & \varepsilon(\mathbf{k}+\mathbf{Q})+h\sigma_z+\alpha\mathcal{L}_0(\mathbf{k}+\mathbf{Q})\cdot\sigma_x\sigma\sigma_x\end{pmatrix} \tag{63}$$

and $\Psi^T_{\mathbf{k}}=(c_{\mathbf{k}\uparrow},c_{\mathbf{k}\downarrow},c_{\mathbf{k}+\mathbf{Q}\downarrow},c_{\mathbf{k}+\mathbf{Q}\uparrow})$. In the following, we assume the perfect nesting condition of the energy band $\varepsilon(\mathbf{k}+\mathbf{Q})=-\varepsilon(\mathbf{k})$. This situation is realized in the case of the half-filling electron density for our model on the square lattice with the nearest-neighbor hopping. The nesting vector is $\mathbf{Q}=(\pm\pi,\pm\pi)$. Furthermore, we postulate $\mathcal{L}_0(\mathbf{k}+\mathbf{Q})=\mathcal{L}_0(\mathbf{k})$. This condition is satisfied when $\mathcal{L}_0(\mathbf{k})=(\sin 2k_y,-\sin 2k_x)$ in the case of $\mathbf{Q}=(\pm\pi,\pm\pi)$. Then, Hamiltonian (63) has the same form as that of the Rashba s-wave superconductor considered in the previous sections, and topological order is realized when the condition $h>\Delta_S$ is fulfilled.

In a similar manner as Sec. V, topological numbers of the SDW state are calculated. The energy gap of the system closes one of the following conditions are satisfied:

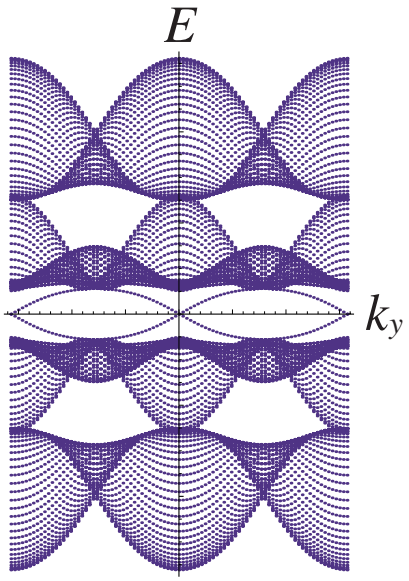

FIG. 10. (Color online) The energy spectra of the NCS CDW state with edges at $i_x=0$ and $i_x=30$. Here k_y denotes the momentum in the y direction and $k_y \in [-\pi, \pi]$. We take $t=1$, $\mu=0$, $\lambda=0.5$, and $\Delta_C=1$. The Zeeman magnetic field H_z is $\mu_B H_z=1.5$.

$$\Delta_S^2 = (\mu_B H_z)^2, \quad 4t^2 + \Delta_S^2 = (\mu_B H_z)^2, \quad 16t^2 + \Delta_S^2 = (\mu_B H_z)^2 \tag{64}$$

and the winding number $I(k_y)$ is calculated as

$$I(k_y) = \frac{1}{2}\{\mathrm{sgn}[\varepsilon(-\pi/2,k_y)^2 - (\mu_B H_z)^2 + \Delta_S^2] - \mathrm{sgn}[\varepsilon(0,k_y)^2 - (\mu_B H_z)^2 + \Delta_S^2] + \mathrm{sgn}[\varepsilon(\pi/2,k_y)^2 - (\mu_B H_z)^2 + \Delta_S^2] - \mathrm{sgn}[\varepsilon(\pi,k_y)^2 - (\mu_B H_z)^2 + \Delta_S^2]\}. \tag{65}$$

Because $\mathcal{H}^*_{SDW}(-\mathbf{k}) = \mathcal{H}_{SDW}(\mathbf{k})$ at $k_y = 0, \pm\pi/2, \pi$, the winding number $I(k_y)$ is defined at these values of k_y. We summarize the winding number of the SDW state in Table IV. The TKNN integer in the magnetic Brillouin zone, which we denote as I_{mTKNN}, is also given in Table IV.

In a similar manner as s-wave NCS superconductors, gapless edge modes appear in the NCS SDW state considered above when $h > \Delta_S$. See Fig. 9. However, in comparison with the case of s-wave superconductivity, we should taken into account only half of the zero-energy modes, since the Brillouin zone is folded to the magnetic Brillouin zone in the SDW state, and as a result, the $\mathbf{k}$ point $\mathbf{k}=(\pi,0)$ is equivalent to $\mathbf{k}=(0,\pi)$. In other words, when $(-1)^{I_{mTKNN}}=-1$, we have odd numbers of zero-energy edge modes in the SDW state. In Fig. 9, we see three zero-energy modes. The existence of odd numbers of zero-energy edge modes implies that in the vortex core of the SDW order $\Delta_S e^{i\theta}$, there are odd numbers of zero-energy modes because of the bulk-edge correspondence. These zero-energy modes have $U(1)$ charge. As in the case of the Su-Schrieffer-Heager model,[42] these isolated zero-energy modes with $U(1)$ charge lead to the charge fractionalization.[43] That is, when these three zero modes are occupied by electrons, the charge carried by the vortex core is $Q=3e/2$.

B. Topological charge-density wave state

The above consideration for the topological SDW state is also applicable to the CDW state. We consider the CDW state with the order parameter $\Delta_C = \langle c^\dagger_{\mathbf{k}\uparrow} c_{\mathbf{k}+\mathbf{Q}\uparrow}\rangle = \langle c^\dagger_{\mathbf{k}\downarrow} c_{\mathbf{k}+\mathbf{Q}\downarrow}\rangle$ in the case with the Rashba SO interaction. The mean-field Hamiltonian for the Rashba CDW state is

$$\mathcal{H}_{CDW} = \frac{1}{2}\sum_{\mathbf{k}} \Psi^\dagger_{C\mathbf{k}} \mathcal{H}_{CDW}(\mathbf{k}) \Psi_{C\mathbf{k}} \tag{66}$$

with

$$\mathcal{H}_{CDW}(\mathbf{k}) = \begin{pmatrix} \varepsilon(\mathbf{k}) - h\sigma_z + \alpha \mathcal{L}_0(\mathbf{k})\cdot\boldsymbol{\sigma} & i\Delta_C\sigma_y \\ -i\Delta_C\sigma_y & \varepsilon(\mathbf{k}+\mathbf{Q}) + h\sigma_z + \alpha\mathcal{L}_0(\mathbf{k}+\mathbf{Q})\cdot\boldsymbol{\sigma}^* \end{pmatrix} \tag{67}$$

and $\Psi^T_{C\mathbf{k}} = (c_{\mathbf{k}\uparrow}, c_{\mathbf{k}\downarrow}, -c_{\mathbf{k}+\mathbf{Q}\downarrow}, c_{\mathbf{k}+\mathbf{Q}\uparrow})$. We assume the prefect nesting condition $\varepsilon(\mathbf{k}+\mathbf{Q}) = -\varepsilon(\mathbf{k})$ again, and also assume that $\mathcal{L}_0(\mathbf{k}+\mathbf{Q}) = -\mathcal{L}_0(\mathbf{k})$. The condition for $\mathcal{L}_0(\mathbf{k})$ is satisfied when $\mathcal{L}_0(\mathbf{k}) = (\sin k_y, -\sin k_x)$ in the case of $\mathbf{Q}=(\pm\pi, \pm\pi)$. Equation (67) is formally equivalent to the Hamiltonian of the Rashba s-wave superconductor. In this CDW state, the topological ordered phase with a single gapless edge mode realizes. We depict an example of the energy spectra for the system with open boundary edges in the case of $h > \Delta_C$ in Fig. 10. There are two zero-energy edge modes at $k_y=0$ and π. Since the Brillouin zone is folded by the CDW order with the ordering vector $\mathbf{Q}=(\pi,\pi)$, the zero mode at $k_y=\pi$ is equivalent to that at $k_y=0$. Thus there is only one zero mode. In this Abelian topological phase, the charge fractionalization can occur, as in the case of the NCS SDW state. When there is a vortex of the CDW order, the zero mode of which is occupied by one electron, the vortex carries the fractional charge $e/2$.

IX. DISCUSSION AND CONCLUSION

A. Realization scheme for the non-Abelian topological order in spin-singlet superconductors

In this section, we discuss possible realization schemes for the non-Abelian topological order considered in the pre-

TABLE IV. The TKNN integer in the magnetic BZ, I_{mTKNN}, and the winding number $I(k_y)$ for 2D SDW state.

$(\mu_B H_z)^2$	$(-1)^{I_{\mathrm{mTKNN}}}$	$I(0)=I(\pi)$	$I(\pi/2)=I(-\pi/2)$
$0<(\mu_B H_z)^2<\Delta_S^2$	1	0	0
$\Delta_S^2<(\mu_B H_z)^2<4t^2+\Delta_S^2$	−1	1	2
$4t^2+\Delta_S^2<(\mu_B H_z)^2<16t^2+\Delta_S^2$	−1	−1	0
$16t^2+\Delta_S^2<(\mu_B H_z)^2$	1	0	0

vious sections. Recently, it was discussed by several authors that *s*-wave Rashba superconductors with the condition $\mu_B H_z > \Delta$ are realizable in heterostructure semiconductor devices.[27,28] We, here, present two more possible schemes; one based on quasi-two-dimensional bulk superconductors and the other utilizing ultracold atoms.[26]

1. Possible realization in strongly correlated electron systems

The most crucial hurdle for the realization of the non-Abelian topological order in the Rashba superconductors is to stabilize the superconducting state under applied strong magnetic fields $\mu_B H_z > \Delta$. As mentioned before, the Pauli depairing effect due to magnetic fields is absent when the SO splitting of the Fermi surface is sufficiently larger than the superconducting gap and the Zeeman energy.[33,35] Such large SO interactions are typically realized in noncentrosymmetric materials. Then, the issue which should be addressed here is how to suppress the orbital depairing effect of magnetic fields. The typical size of the orbital limiting field H_{c2}^{orb} is given by $\mu_B H_{c2}^{\mathrm{orb}} \sim \Delta^2/(zE_F)$. Here z is the mass normalization factor. If the mass enhancement factor $1/z$ is sufficiently large, it is possible to attain $\mu_B H_{c2}^{\mathrm{orb}} > \Delta$. For instance, for strongly correlated electron systems such heavy fermion superconductors, $1/z$ can reach to be ~ 100. Thus, it is not difficult to fulfill the condition $\mu_B H_{c2}^{\mathrm{orb}} > \Delta$ even when $\Delta/E_F \sim 0.01$. The above argument implies that noncentrosymmetric heavy fermion superconductors may be good candidates for the realization of the non-Abelian topological order. Unfortunately, to this date, there are no noncentrosymmetric heavy fermion superconductors with no gap nodes. Experimental studies suggest that all heavy fermion superconductors without inversion symmetry discovered so far such as $CePt_3Si$ and $CeRh(Ir)Si_3$ possess nodes of the superconducting gap,[44–49] excitations from which may destabilize the topological order.

2. Possible realization in ultracold fermionic atoms

We now discuss an experimental scheme for the realization of the non-Abelian topological order in ultracold fermionic atoms. We can use the Feshbach resonance in the *s*-wave channel for the formation of the *s*-wave Cooper pairs in this system.[50,51] For superfluid states of charge neutral atoms, there is no orbital depairing effect due to applied magnetic fields. Moreover, it was recently proposed by several authors that effective SO interactions acting on charge neutral atoms can be generated by spatially varying laser fields.[52–55] When the effective SO interaction is the Rashba type (or more generally, antisymmetric), and its magnitude is sufficiently larger than the Zeeman energy due to an applied magnetic field, the Pauli depairing effect is suppressed, as mentioned before. Thus, the condition for the non-Abelian topological order $\mu_B H_z > \Delta$ can be easily fulfilled. As discussed in the previous sections, the non-Abelian anyons are stable for sufficiently low energies $\ll \min\{\mu_B H_z - \Delta, \Delta\}$. Since the BCS gap Δ can be tuned to be large, i.e., $\Delta \sim E_F$, by using the *s*-wave Feshbach resonance, the realization of the non-Abelian anyons in this scheme is quite promising. In the following, we present two schemes for the realization of the topological phase in ultracold fermionic atoms with laser generated SO interaction.

The first scheme utilizes an optical lattice with laser-assisted tunneling of fermionic atoms. We consider fermionic atoms loaded in a 2D periodic optical lattice.[52] The atoms occupy doubly degenerate Zeeman levels of the hyperfine ground state manifolds, which correspond to the spin-up and spin-down states of electrons. We introduce the Zeeman field to lift the degeneracy. We assume that standard tunneling of atoms between sites due to kinetic energy is suppressed by the large depth of the optical lattice potential. Tunneling of atoms between neighboring sites along the ν direction ($\nu = x, y$) which conserves spins is caused by laser beams via optical Raman transitions.[52,56] In addition, tunneling which accompanies spin flip is also driven by two Raman lasers.[52] The Rabi frequency of the laser $\Omega_{\nu 1}$ ($\Omega_{\nu 2}$) is resonant for transition from the spin-up state to the spin-down state for the tunneling between neighboring sites in the forward (backward) ν direction. Furthermore, the confining optical potential is tilted along both the x direction and the y direction to assure that the forward and backward tunneling processes are, respectively, induced by the lasers with the different Rabi frequencies $\Omega_{\nu 1}$ and $\Omega_{\nu 2}$. The tilting potential for the x direction Δ_x is different from that for y direction Δ_y to ensure that tunneling accompanying spin flip along the $y(x)$ direction is not raised by the lasers with $\Omega_{x(y)1,2}$. It is also assumed that the detuning from excited states for optical Raman transitions is much larger than $\Delta_{x(y)}$, and thus the spatial variation in the amplitudes of the Rabi frequencies due to the tilting potential is negligible. To realize the Rashba SO interaction for the two Zeeman levels, we choose the phases of the lasers as follows. The lasers are propagating along the z direction with an oscillating factor $e^{ik_z z}$. The Rabi frequency Ω_{x2} is expressed as $\Omega_{x2} = |\Omega_{x2}| e^{ik_z z}$. The phase of the laser Ω_{x1} is shifted by π from that of Ω_{x2}, and $\Omega_{x2} = -\Omega_{x1}$ holds. The phase of Ω_{y1} (Ω_{y2}) is shifted by $-\pi/2$ ($\pi/2$), and $\Omega_{y2} = -i\Omega_{x1}$, $\Omega_{y2} = -\Omega_{y1}$. Then, the laser-induced tunneling term which accompanies spin flip is expressed by

$$\mathcal{H}_{\mathrm{SO}} = \sum_i [\alpha_x(c^\dagger_{\mathbf{i}-\hat{x}\downarrow}c_{\mathbf{i}\uparrow} - c^\dagger_{\mathbf{i}+\hat{x}\downarrow}c_{\mathbf{i}\uparrow}) + i\alpha_y(c^\dagger_{\mathbf{i}-\hat{y}\downarrow}c_{\mathbf{i}\uparrow} - c^\dagger_{\mathbf{i}+\hat{y}\downarrow}c_{\mathbf{i}\uparrow}) + \mathrm{H.c.}],$$

$$\alpha_\nu = c_\nu \int d\mathbf{r}\psi^*_\downarrow(\mathbf{r}-\mathbf{r}_{i-\hat{\mu}})\Omega_{\nu 2}(\mathbf{r})\psi_\uparrow(\mathbf{r}-\mathbf{r}_i) \tag{68}$$

with $\nu=x$, y, and $c_x=1$ and $c_y=-i$. Since we consider the 2D xy plane with $z=0$, α_ν is real. For $\alpha_x=\alpha_y$, Eq. (68) is the Rashba SO interaction.

In the second scheme, we employ the idea that an effective SO interaction is created by utilizing the dark states generated by spatially varying laser fields, as proposed in Refs. 53 and 55. We can introduce a vortex of the superfluid order parameter by changing the topology of the shape of a trapping potential. Since the underlying topological effective field theory is the $SU(2)_2$ Chern-Simons theory,[3,4,57] a vortex with a zero-energy Majorana mode is equivalent to a hole pierced in the system provided that the total number of the holes in the system are odd. The trapping potential with holes can be prepared by using a holographically engineered laser technique.[58] Furthermore, the dynamical motions of holes are possible through a computer-generated hologram; i.e., the positions of holes can be moved by changing temporally the shape of the confining potential which may be achieved by preprogrammed hologram. Remarkably, this enables the braiding of vortices (holes), which amounts to a quantum gate for fault-tolerant quantum computation based on the manipulation of non-Abelian anyons.[12,13]

B. Conclusion

We have verified that the non-Abelian topological order, which is characterized by the existence of chiral Majorana edge modes and a Majorana fermion in a vortex core, can be realized in almost all classes of fully gapped spin-singlet superconductors with antisymmetric SO interactions such as the Rashba SO interaction in the case with the Zeeman magnetic field. Majorana fermions in superconductors have been, recently, attracting much attention in connection with the topological quantum computation. The idea of the topological quantum computation has been examined for the non-Abelian fractional quantum Hall state,[12,14] spin-triplet chiral p-wave superconductors,[17] and the proximity between a topological insulator and a conventional superconductor.[23,41] Our results in the present paper provide another category of promising systems for the realization of the topological quantum computation. We would like to stress that our systems in the normal state are topologically trivial; i.e., the combination of the conventional superconducting order and the conventional antisymmetric SO interaction with the Zeeman field gives rise to a highly nontrivial topological phase. In our scenario, the existence of the Zeeman energy, the magnitude of which exceeds the size of the superconducting gap opened at time-reversal invariant $\mathbf{k}$ points in the Brillouin zone where the SO interaction vanishes, is important. At these $\mathbf{k}$ points, there are Dirac cones in the absence of magnetic fields. When the magnetic field is switched on, the effective gap of electrons in the vicinity of the Dirac cone is given by $\Delta-\mu_B H_z$. As the magnetic field increases, and $\mu_B H_z$ exceeds Δ, the sign of the effective gap changes, and topological phase transition occurs. As indicated by the analysis of Majorana fermion modes in open boundary edges and in a vortex core in Secs. VI and VII, and in the topological argument based on the winding number in Sec. V, quasiparticles in the vicinity of the Dirac cone, i.e., time-reversal invariant $\mathbf{k}$ points, play an important role for the realization of the topological quantum phase transition. In the case of the s-wave pairing state, the large magnetic field satisfying $\mu_B H_z > \Delta$ is required to realize the non-Abelian topological order. For conventional bulk weak-coupling superconductors, it is difficult to fulfill this condition, though there are some proposals to realize this system in heterostructure devices, for which $\mu_B H_z > \Delta$ is attainable.[27,28] We have proposed promising schemes for the realization of the condition $\mu_B H_z > \Delta$ in the bulk s-wave pairing state; one based on strongly correlated electron systems and the other utilizing ultracold fermionic atoms.[26] In contrast to the s-wave pairing state, in the case of the $d+id$ wave pairing state, a small magnetic field larger than the lower critical field is sufficient to fulfill the condition $\mu_B H_z > \Delta_k$ in the vicinity of time-reversal invariant $\mathbf{k}$ points, and thus the realization of the non-Abelian topological phase is easier than the s-wave case. However, unfortunately, up to our knowledge, there is no superconductor for which the $d+id$-wave pairing state is experimentally established, though it was suggested by some authors that this pairing state may be realized in sodium cobalt oxide superconductors $Na_xCoO_2 \cdot yH_2O$.[59,60] It is an interesting open issue to pursue the experimental detection of Majorana fermions in such superconductors mentioned above. We have also clarified that, in certain parameter regions, the Majorana fermion realized in Rashba spin-singlet superconductors is stable against various sources of decoherence such as thermal fluctuations which exist in real systems generically. Because of this feature, the Rashba spin-singlet superconductor may be a promising candidate for the realization of the topological quantum computation.

As a by-product of our analysis, we have also found that an Abelian topological order, which supports the existence of gapless Dirac fermions in edges and the charge fractionalization, is realizable in the conventional SDW or CDW state with an antisymmetric SO interaction.

ACKNOWLEDGMENTS

The authors thank S. Das Sarma for discussions. M.S. would like to thank Y. Tanaka for discussions. This work is partly supported by the Sumitomo Foundation (M.S.) and the Grant-in-Aids for Scientific Research from the Minestry of Education, Culture, Sports, Science and Technology of Japan [Grants No. 19052003, No. 21102510 (S.F.), and No. 22540383 (M.S.)].

APPENDIX A: TKNN NUMBER AND THE DUAL TRANSFORMATION

In this appendix, we show that the dual transformation [Eq. (11)] does not change the TKNN number, and hence the

topological properties of the original Hamiltonian (4) and the dual Hamiltonian (11) are the same. Let us consider the BdG equations for the original Hamiltonian $\mathcal{H}(\mathbf{k})$ and that for the dual one $\mathcal{H}_{\mathrm{D}}(\mathbf{k})$,

$$\mathcal{H}(\mathbf{k})|\phi_n(\mathbf{k})\rangle = E_n(\mathbf{k})|\phi_n(\mathbf{k})\rangle,$$

$$\mathcal{H}_{\mathrm{D}}(\mathbf{k})|\phi_n^{\mathrm{D}}(\mathbf{k})\rangle = E_n(\mathbf{k})|\phi_n^{\mathrm{D}}(\mathbf{k})\rangle. \tag{A1}$$

Since the dual transformation is a unitary transformation, the energy spectrum of the dual Hamiltonian is the same as that of the original one. Moreover, the eigenstate $|\phi_n^{\mathrm{D}}(\mathbf{k})\rangle$ for the dual Hamiltonian is related to the eigenstate $|\phi_n(\mathbf{k})\rangle$ for the original one as

$$|\phi_n^{\mathrm{D}}(\mathbf{k})\rangle = D|\phi_n(\mathbf{k})\rangle \tag{A2}$$

with D in Eq. (12). As D is a constant unitary matrix, the gauge field constructed from the occupied states for the dual Hamiltonian is the same as that for the original one,

$$\begin{aligned} A_i^{(-)\mathrm{D}}(\mathbf{k}) &= i \sum_{E_n(\mathbf{k})<0} \langle \phi_n^{\mathrm{D}}(\mathbf{k})|\partial_{k_i}\varphi_n^{\mathrm{D}}(\mathbf{k})\rangle \\ &= i \sum_{E_n(\mathbf{k})<0} \langle \phi_n(\mathbf{k})|\partial_{k_i}\phi_n(\mathbf{k})\rangle = A_i^{(-)}(\mathbf{k}). \end{aligned} \tag{A3}$$

This relation immediately means that the TKNN number [Eq. (15)] is invariant under the dual transformation.

APPENDIX B: TKNN NUMBER AND WINDING NUMBER

1. TKNN number for TRB topological superconductors

In this appendix, we summarize useful properties of the TKNN number for TRB topological superconductors.[22] Let us first consider the BdG equation,

$$\mathcal{H}(\mathbf{k})|\phi_n(\mathbf{k})\rangle = E_n(\mathbf{k})|\phi_n(\mathbf{k})\rangle, \tag{B1}$$

where the BdG Hamiltonian $\mathcal{H}(\mathbf{k})$ has the particle-hole symmetry,

$$\Gamma\mathcal{H}(\mathbf{k})\Gamma^{\dagger} = -\mathcal{H}(-\mathbf{k})^{*} \tag{B2}$$

with the 4×4 matrix Γ

$$\Gamma = \begin{pmatrix} 0 & 1_{2\times2} \\ 1_{2\times2} & 0 \end{pmatrix}. \tag{B3}$$

From the particle-hole symmetry, we can say that if $|\phi_n(\mathbf{k})\rangle$ is a positive energy state with $E_n(\mathbf{k})>0$, then $\Gamma|\phi_n^{*}(-\mathbf{k})\rangle$ is a negative energy state with $-E_n(-\mathbf{k})$. Therefore, in the following, we use a positive (negative) n to represent a positive (negative) energy state, and set

$$|\phi_{-n}(\mathbf{k})\rangle = \Gamma|\phi_n^{*}(-\mathbf{k})\rangle. \tag{B4}$$

For the ground state in a superconductor, the negative energy states are occupied.

Now we introduce the following "gauge fields" $A_i^{(\pm)}(\mathbf{k})$:

$$A_i^{(\pm)} = i\sum_{n\gtrless0} \langle \phi_n(\mathbf{k})|\partial_{k_i}\phi_n(\mathbf{k})\rangle. \tag{B5}$$

From Eq. (B4), the gauge fields $A_i^{(\pm)}(\mathbf{k})$ satisfy

$$A_i^{(+)}(\mathbf{k}) = A_i^{(-)}(-\mathbf{k}). \tag{B6}$$

It is also found that their sum $A_i(\mathbf{k}) \equiv A_i^{(+)}(\mathbf{k}) + A_i^{(-)}(\mathbf{k})$ is given by a total derivative of a function. To see this, we rewrite $|\phi_n(\mathbf{k})\rangle$ in the components,

$$|\phi_n(\mathbf{k})\rangle = \begin{pmatrix} \phi_n^1(\mathbf{k}) \\ \phi_n^2(\mathbf{k}) \\ \phi_n^3(\mathbf{k}) \\ \phi_n^4(\mathbf{k}) \end{pmatrix} \tag{B7}$$

and introduce the 4×4 unitary matrix $W(\mathbf{k})$ as

$$W_{a,n}(\mathbf{k}) = \phi_n^a(\mathbf{k}). \tag{B8}$$

Then $A_i(\mathbf{k})$ is rewritten as the total derivative of $i\ \ln[\det W(\mathbf{k})]$,

$$A_i(\mathbf{k}) = i\ \mathrm{tr}[W^{\dagger}(\mathbf{k})\partial_{k_i}W(\mathbf{k})] = i\partial_{k_i}\ \ln[\det W(\mathbf{k})]. \tag{B9}$$

This equation implies that the field strength of $A_i(\mathbf{k})$ is identically zero,

$$\mathcal{F}(\mathbf{k}) = \epsilon^{ij}\partial_{k_i}A_j(\mathbf{k}) = 0. \tag{B10}$$

Combining this with Eq. (B6), we find that the field strength $\mathcal{F}^{(\pm)}(\mathbf{k})$ of $A_i^{(\pm)}(\mathbf{k})$ satisfies

$$\mathcal{F}^{(\pm)}(\mathbf{k}) = \mathcal{F}^{(\pm)}(-\mathbf{k}). \tag{B11}$$

By using the field strength of the occupied state, the TKNN number is define as

$$I_{\mathrm{TKNN}} = \frac{1}{2\pi}\int_{T^2} d^2k\mathcal{F}^{(-)}(\mathbf{k}), \tag{B12}$$

where T^2 is the first Brillouin zone in the momentum space. Using relation (B11) and the Stokes' theorem, we obtain

$$\begin{aligned} I_{\mathrm{TKNN}} &= \frac{1}{\pi}\int_{T_+^2} d^2k\mathcal{F}^{(-)}(\mathbf{k}) \\ &= \frac{1}{\pi}\left[\int_{-\pi}^{\pi} dk_x A_x^{(-)}(k_x,0) - \int_{-\pi}^{\pi} dk_x A_x^{(-)}(k_x,\pi)\right], \end{aligned} \tag{B13}$$

where T_+^2 is the upper half plane of T^2. As is shown in Appendix B 3, this formula enables us to connect the Chern number to the winding number defined in Eq. (21).

2. Winding number

As was discussed in Sec. V, the winding number $I(k_y)$ is defined by taking the basis where the BdG Hamiltonian has the following particular form:[21]

$$\mathcal{H}(\mathbf{k}) = \begin{pmatrix} 0 & q(\mathbf{k}) \\ q^\dagger(\mathbf{k}) & 0 \end{pmatrix}. \tag{B14}$$

By using $q(\mathbf{k})$, the winding number is defined as

$$I(k_y) = \frac{1}{4\pi i}\int_{-\pi}^{\pi} dk_x \, \mathrm{tr}[q^{-1}(\mathbf{k})\partial_{k_x} q(\mathbf{k}) - q^{\dagger -1}(\mathbf{k})\partial_{k_x} q^\dagger(\mathbf{k})], \tag{B15}$$

which is equivalently rewritten as

$$I(k_y) = -\frac{1}{2\pi i}\int_{-\pi}^{\pi} dk_x \, \mathrm{tr}[q(\mathbf{k})\partial_{k_i} q^{-1}(\mathbf{k})]$$

$$= \frac{1}{2\pi i}\int_{-\pi}^{\pi} dk_x \partial_{k_i} \ln[\det q(\mathbf{k})]. \tag{B16}$$

Now we derive a useful formula to evaluate the winding number $I(k_y)$. Denote the real and imaginary parts of $\det q(\mathbf{k})$ as $m_1(\mathbf{k})$ and $m_2(\mathbf{k})$, respectively,

$$\det q(\mathbf{k}) = m_1(\mathbf{k}) + i m_2(\mathbf{k}). \tag{B17}$$

Then, $I(\mathbf{k})$ is rewritten as

$$I(\mathbf{k}) = \frac{1}{2\pi}\int_{-\pi}^{\pi} dk_x \epsilon^{ij}\hat{m}_i(\mathbf{k})\partial_{k_x}\hat{m}_j(\mathbf{k}), \tag{B18}$$

where $\hat{m}_i(\mathbf{k})$ is given by

$$\hat{m}_i(\mathbf{k}) = \frac{m_i(\mathbf{k})}{\sqrt{m_1(\mathbf{k})^2 + m_2(\mathbf{k})^2}}. \tag{B19}$$

To evaluate Eq. (B18), we use the technique developed in Ref. 61. From the topological nature of $I(k_y)$, we can rescale one of $m_i(\mathbf{k})$'s, say $m_1(\mathbf{k})$, as $m_1(\mathbf{k}) \to a m_1(\mathbf{k})$ $(a \ll 1)$ without changing the value of $I(k_y)$. Then it is found that only neighborhoods of k_x^0 satisfying $m_2(k_x^0, k_y) = 0$ contribute to $I(k_y)$ if a is small enough. By expanding $m_i(\mathbf{k})$ as

$$m_1(\mathbf{k}) = m_1(k_x^0, k_y) + \cdots,$$

$$m_2(\mathbf{k}) = \partial_{k_x} m_2(k_x^0, k_y)(k_x - k_x^0) + \cdots, \tag{B20}$$

the contribution from k_x^0 is calculated as

$$\frac{1}{2}\mathrm{sgn}[m_1(k_x^0, k_y)] \cdot \mathrm{sgn}[\partial_{k_x} m_2(k_x^0, k_y)]. \tag{B21}$$

Summing up the contribution of all zeros, we obtain

$$I(k_y) = \sum_{\{k_x^0 : m_2(k_x^0, k_y) = 0\}} \frac{1}{2}\mathrm{sgn}[m_1(k_x^0, k_y)] \cdot \mathrm{sgn}[\partial_{k_x} m_2(k_x^0, k_y)]. \tag{B22}$$

Exchanging $m_1(\mathbf{k})$ with $m_2(\mathbf{k})$ in the above argument, we also have

$$I(k_y) = -\sum_{\{k_x^0 : m_1(k_x^0, k_y) = 0\}} \frac{1}{2}\mathrm{sgn}[\partial_{k_x} m_1(k_x^0, k_y)] \cdot \mathrm{sgn}[m_2(k_x^0, k_y)]. \tag{B23}$$

3. Relation between the TKNN number and the winding number

Here we prove relation (22) between the TKNN number and the winding number. As was shown in Eq. (B13), the TKNN number for a TRB superconductor is evaluated by the line integral

$$\frac{1}{\pi}\int_{-\pi}^{\pi} dk_x A_i^{(-)}(k_x, k_y) \tag{B24}$$

with $k_y = 0$ or $k_y = \pi$. From the particle-hole symmetry, this line integral itself is a $\mathbf{Z}_2$ topological number.[22,62] In this section, we relate this line integral to the winding number defined in the previous section.

First, consider the eigenequation

$$q(\mathbf{k})q^\dagger(\mathbf{k})|u_n(\mathbf{k})\rangle = E_n(\mathbf{k})^2|u_n(\mathbf{k})\rangle, \tag{B25}$$

where $q(\mathbf{k})$ is given by an off-diagonal component of Hamiltonian (B14). Using the components of $|u_n(\mathbf{k})\rangle$,

$$|u_n(\mathbf{k})\rangle = \begin{pmatrix} u_n^1(\mathbf{k}) \\ u_n^2(\mathbf{k}) \end{pmatrix}, \tag{B26}$$

we define the 2×2 unitary matrix $U(\mathbf{k})$,

$$U(\mathbf{k})_{a,n} = u_n^a(\mathbf{k}). \tag{B27}$$

Then the eigenequation is recast into

$$q(\mathbf{k})q^\dagger(\mathbf{k})U(\mathbf{k}) = U(\mathbf{k})\Lambda(\mathbf{k}), \tag{B28}$$

where $\Lambda(\mathbf{k})$ is given by

$$\Lambda(\mathbf{k}) = \mathrm{diag}[E_1(\mathbf{k})^2, E_2(\mathbf{k})^2]. \tag{B29}$$

Equation (B28) yields

$$q^{-1}(\mathbf{k}) = q^\dagger(\mathbf{k})U(\mathbf{k})\Lambda^{-1}(\mathbf{k})U^\dagger(\mathbf{k}). \tag{B30}$$

By using $q(\mathbf{k})$ and $|u_n(\mathbf{k})\rangle$ in the above, the occupied state $|\phi_n^{(-)}(\mathbf{k})\rangle$ of Hamiltonian (B14) is given by

$$|\phi_n^{(-)}(\mathbf{k})\rangle = \frac{1}{\sqrt{2}}\begin{pmatrix} |u_n(\mathbf{k})\rangle \\ q^\dagger(\mathbf{k})|u_n(\mathbf{k})\rangle/E_n(\mathbf{k}) \end{pmatrix}, \tag{B31}$$

with negative n. Here $|u_n(\mathbf{k})\rangle$ is normalized as $\langle u_n(\mathbf{k})|u_n(\mathbf{k})\rangle = 1$. Thus the gauge field $A_i^{(-)}(\mathbf{k})$ is calculated as

$$A_i^{(-)}(\mathbf{k}) = i\sum_{n<0}\langle\phi_n^{(-)}(\mathbf{k})|\partial_{k_i}\phi_n^{(-)}(\mathbf{k})\rangle$$

$$= i\sum_{n<0}\langle u_n(\mathbf{k})|\partial u_n(\mathbf{k})\rangle + i\sum_{n<0}\frac{1}{2E_n(\mathbf{k})^2}u_n^{a*}(\mathbf{k})q_{ab}(\mathbf{k})$$

$$\times\partial_{k_i}q_{bc}^\dagger(\mathbf{k})u_n^c(\mathbf{k}) + i\sum_{n<0}\frac{1}{2}E_n(\mathbf{k})\partial_{k_i}\left[\frac{1}{E_n(\mathbf{k})}\right]$$

$$= i\,\mathrm{tr}[U^\dagger(\mathbf{k})\partial_{k_i}U(\mathbf{k})]$$

$$+ i\frac{1}{2}\mathrm{tr}[q(\mathbf{k})\partial_{k_i}q^\dagger U(\mathbf{k})\Lambda^{-1}(\mathbf{k})U^\dagger(\mathbf{k})]$$

$$+ i\sum_{n<0}\frac{1}{2}E_n(\mathbf{k})\partial_{k_i}\left[\frac{1}{E_n(\mathbf{k})}\right]$$

$$= i\,\mathrm{tr}[U^{\dagger}(\mathbf{k})\partial_{k_i}U(\mathbf{k})] + i\frac{1}{2}\mathrm{tr}[q(\mathbf{k})\partial_{k_i}q^{-1}(\mathbf{k})] + i\frac{1}{2}\sum_{n<0}\partial_{k_i}\ln E_n(\mathbf{k}), \tag{B32}$$

where we have used Eq. (B30) in the last line of the above equation. We also notice here that the unitary transformation used to obtain the Hamiltonian in form (B14) is accomplished by a constant unitary matrix, so it does not change the value of $A_i^{(-)}(\mathbf{k})$. Substituting this into Eq. (B13), we obtain

$$I_{\mathrm{TKNN}} = I(0) - I(\pi) + \frac{i}{\pi}\int_{-\pi}^{\pi} dk_x\,\mathrm{tr}[U^{\dagger}(\mathbf{k})\partial_{k_x}U(\mathbf{k})]|_{k_y=0} - \frac{i}{\pi}\int_{-\pi}^{\pi} dk_x\,\mathrm{tr}[U^{\dagger}(\mathbf{k})\partial_{k_x}U(\mathbf{k})]|_{k_y=\pi}. \tag{B33}$$

Since we have

$$\frac{i}{\pi}\int_{-\pi}^{\pi} dk_x\,\mathrm{tr}[U^{\dagger}(\mathbf{k})\partial_{k_x}U(\mathbf{k})] = \frac{i}{\pi}\int_{-\pi}^{\pi} dk_x\partial_{k_x}\ln\det U(\mathbf{k}) = 2N, \tag{B34}$$

with an integer N, the last two terms in the right-hand side of Eq. (B33) are even integers. Therefore, we obtain

$$(-1)^{I_{\mathrm{TKNN}}} = (-1)^{I(0)-I(\pi)}. \tag{B35}$$

APPENDIX C: TKNN NUMBER AND CHIRALITY BASIS

In Sec. V, it is discussed that the origin of the non-Abelian topological order in spin-singlet Rashba superconductors is understood in terms of mapping to spinless odd-parity superconductors which is derived from the chirality basis representation. This mapping was first considered in Ref. 63, though the parameter region in which this mapping is applicable was not fully elucidated in Ref. 63. Actually, this mapping can be used when the Zeeman energy is much larger than the superconducting gap. In this appendix, we will show that this mapping does not change the topological number of the original system. This property is not trivial since the mapping depends on wave numbers and hence the band structure of electrons in a nontrivial way.

1. Chirality basis

For simplicity, we suppose that $\mu_{\mathrm{B}}H_z > 0$ in the following. In our Hamiltonian (4), the normal dispersion of electron is determined by

$$\mathcal{E}(\mathbf{k}) = \varepsilon(\mathbf{k}) - \mu_{\mathrm{B}}H_z\sigma_z + \alpha\mathcal{L}_0(\mathbf{k})\cdot\boldsymbol{\sigma}. \tag{C1}$$

In the chirality basis, it is diagonalized as

$$\mathcal{E}(\mathbf{k}) = U(\mathbf{k})\begin{pmatrix}\varepsilon_+(\mathbf{k}) & 0\\ 0 & \varepsilon_-(\mathbf{k})\end{pmatrix}U^{\dagger}(\mathbf{k}), \tag{C2}$$

where $\varepsilon_{\pm}(\mathbf{k}) = \varepsilon(\mathbf{k}) \pm \Delta\varepsilon(\mathbf{k})$, and $\Delta\varepsilon(\mathbf{k})$ is given by

$$\Delta\varepsilon(\mathbf{k}) = \sqrt{[\alpha\mathcal{L}_0(\mathbf{k})]^2 + (\mu_{\mathrm{B}}H_z)^2}, \tag{C3}$$

and $U(\mathbf{k})$ is

$$U(\mathbf{k}) = \frac{1}{\sqrt{2\Delta\varepsilon(\mathbf{k})[\Delta\varepsilon(\mathbf{k}) + \mu_{\mathrm{B}}H_z]}}\begin{pmatrix}\alpha\mathcal{L}_{0x}(\mathbf{k}) - i\alpha\mathcal{L}_{0y}(\mathbf{k}) & -\Delta\varepsilon(\mathbf{k}) - \mu_{\mathrm{B}}H_z\\ \Delta\varepsilon(\mathbf{k}) + \mu_{\mathrm{B}}H_z & \alpha\mathcal{L}_{0x}(\mathbf{k}) + i\alpha\mathcal{L}_{0y}(\mathbf{k})\end{pmatrix}. \tag{C4}$$

From the following unitary transformation:

$$\mathcal{H}(\mathbf{k}) = G(\mathbf{k})^{\dagger}\tilde{\mathcal{H}}(\mathbf{k})G(\mathbf{k}) \tag{C5}$$

with

$$G(\mathbf{k}) = \begin{pmatrix}U^{\dagger}(\mathbf{k}) & 0\\ 0 & U^{T}(-\mathbf{k})\end{pmatrix}, \tag{C6}$$

it is found that the BdG Hamiltonian $\tilde{\mathcal{H}}(\mathbf{k})$ in the chirality basis is given by

$$\tilde{\mathcal{H}}(\mathbf{k}) = \begin{pmatrix}\varepsilon(\mathbf{k}) + \Delta\varepsilon(\mathbf{k})\sigma_z & i\Delta(\mathbf{k})[U^{\dagger}(\mathbf{k})\sigma_y U^{*}(-\mathbf{k})]\\ -i\Delta^{*}(\mathbf{k})[U^{T}(-\mathbf{k})\sigma_y U(\mathbf{k})] & -\varepsilon(\mathbf{k}) - \Delta\varepsilon(\mathbf{k})\sigma_z\end{pmatrix}. \tag{C7}$$

Therefore, the gap function $\tilde{\Delta}_{\sigma\sigma'}(\mathbf{k})$ in the chirality basis becomes

$$\tilde{\Delta}_{\sigma\sigma'}(\mathbf{k}) = i\Delta(\mathbf{k})[U^{\dagger}(\mathbf{k})\sigma_y U^{*}(-\mathbf{k})]_{\sigma\sigma'} = \frac{1}{\Delta\varepsilon(\mathbf{k})}\begin{pmatrix}[\alpha\mathcal{L}_{0x}(\mathbf{k}) + i\alpha\mathcal{L}_{0y}(\mathbf{k})]\Delta(\mathbf{k}) & \mu_{\mathrm{B}}H_z\Delta(\mathbf{k})\\ -\mu_{\mathrm{B}}H_z\Delta(\mathbf{k}) & [\alpha\mathcal{L}_{0x}(\mathbf{k}) - i\alpha\mathcal{L}_{0y}(\mathbf{k})]\Delta(\mathbf{k})\end{pmatrix}. \tag{C8}$$

This equation indicates that when the original gap function $\Delta(\mathbf{k})$ is even parity, the odd-parity gap functions [the diagonal terms of Eq. (C8)] are induced in the chirality basis due to the existence of the SO interaction. However, this never means that

the topological class is always the same as that of spin-triplet superconductors because the off-diagonal terms of Eq. (C8) corresponding to the interband pairing may change its topological property. As a matter of fact, the non-Abelian topological order appears when one of the two bands $\varepsilon_{\pm}(\mathbf{k})$ is gapped by the large Zeeman field satisfying $\mu_B H_z \gg |\Delta(\mathbf{k})|$, and only one band survives in the low-energy region. More precisely, in the parameter regions of the non-Abelian phase shown in Tables I–III in Sec. V, when $\mu<0$, the Zeeman term generates a large gap in the band $\varepsilon_+(\mathbf{k})$, leaving only one band $\varepsilon_-(\mathbf{k})$ in the low-energy region, and hence a spinless odd-parity superconductor is realized for the band $\varepsilon_-(\mathbf{k})$. The effective Hamiltonian $\tilde{\mathcal{H}}_-(\mathbf{k})$ for the spinless chiral odd-parity superconductor is obtained by integrating out fermion fields for the high-energy massive band,

$$\tilde{\mathcal{H}}_-(\mathbf{k}) = \begin{pmatrix} \varepsilon_-(\mathbf{k}) & [\alpha\mathcal{L}_{0x}(\mathbf{k}) - i\alpha\mathcal{L}_{0y}(\mathbf{k})][\Delta(\mathbf{k})/\Delta\varepsilon(\mathbf{k})] \\ [\alpha\mathcal{L}_{0x}(\mathbf{k}) + i\alpha\mathcal{L}_{0y}(\mathbf{k})][\Delta^*(\mathbf{k})/\Delta\varepsilon(\mathbf{k})] & -\varepsilon_-(\mathbf{k}) \end{pmatrix}. \tag{C9}$$

In a similar manner, in the non-Abelian phase with $\mu>0$, the Zeeman term generates a large gap in the band $\varepsilon_-(\mathbf{k})$, leaving only one band $\varepsilon_+(\mathbf{k})$ in the low-energy region, and thus, the following spinless odd-parity superconductor is realized for the band $\varepsilon_+(\mathbf{k})$:

$$\tilde{\mathcal{H}}_+(\mathbf{k}) = \begin{pmatrix} \varepsilon_+(\mathbf{k}) & [\alpha\mathcal{L}_{0x}(\mathbf{k}) + i\alpha\mathcal{L}_{0y}(\mathbf{k})][\Delta(\mathbf{k})/\Delta\varepsilon(\mathbf{k})] \\ [\alpha\mathcal{L}_{0x}(\mathbf{k}) - i\alpha\mathcal{L}_{0y}(\mathbf{k})][\Delta^*(\mathbf{k})/\Delta\varepsilon(\mathbf{k})] & -\varepsilon_+(\mathbf{k}) \end{pmatrix}. \tag{C10}$$

In both cases, the Rashba s-wave ($d+id$-wave) superconductor in this situation is mapped into spinless chiral p-wave (f-wave or p-wave) superconductor.

The above consideration based on the chirality basis is also useful for understanding the origin of the Abelian topological order presented in Sec. VIII. The Abelian order realizes in the vicinity of the half filling $\mu\approx 0$. In this case, there are one particlelike band and one holelike band. In addition, there are Dirac cones at $\mathbf{k}=(\pm\pi,0)$ and $(0,\pm\pi)$. When $\mu_B H_z \gg |\Delta(\mathbf{k})|$, the Dirac cone bands have a large gap $\sim\mu_B H_z$, and can be integrated out in the low-energy region. Then, there remain one particlelike band and one holelike band. Furthermore, when $\alpha|\mathcal{L}_0(\mathbf{k})| \gg \mu_B H_z \gg |\Delta(\mathbf{k})|$, the interband pairs [off-diagonal terms of Eq. (C8)] are negligibly small compared to the intraband pairs. Since the chiral gapless edge state associated with $\tilde{H}_+(\mathbf{k})$ which corresponds to the particlelike band and that with $\tilde{H}_-(\mathbf{k})$ corresponding to the holelike band have the same chirality, propagating in the same direction, the perturbation due to the interband pairs does not raise gap in the two edge modes. This implies that the system is mapped to two decoupled spinless chiral odd-parity superconductors for $\alpha|\mathcal{L}_0(\mathbf{k})| \gg \mu_B H_z \gg |\Delta(\mathbf{k})|$.

By contrast, in the parameter regions where there is no topological order, there are two particlelike bands ($\mu<0$) or two holelike bands ($\mu>0$). In such cases, the edge modes associated with $\tilde{H}_+(\mathbf{k})$ and $\tilde{H}_-(\mathbf{k})$ propagate, respectively, in the opposite directions. Thus, even a small perturbation due to the interband pairing terms of Eq. (C8) gives rise to a gap in the edge excitations, and hence there is no topological order.

2. TKNN number in the chirality basis

Here we will show that the unitary transformation [Eq. (C5)] for the chirality basis does not change the TKNN number in the presence of the Zeeman magnetic field, and hence the topological properties of the original Hamiltonian $\mathcal{H}(\mathbf{k})$ and the Hamiltonian $\tilde{\mathcal{H}}(\mathbf{k})$ in the chirality basis are the same.

Let us first rewrite formula (B13) in a more convenient form. Using Eq. (B6), the TKNN number is recast into

$$I_{\mathrm{TKNN}} = \frac{1}{\pi}\int_0^{\pi} dk_x [A_x(k_x,0) - A_x(k_x,\pi)]. \tag{C11}$$

We will use this formula to prove the above statement.

As was shown in Appendix C 1, $\tilde{\mathcal{H}}(\mathbf{k})$ is related to the original Hamiltonian $\mathcal{H}(\mathbf{k})$ as follows:

$$\mathcal{H}(\mathbf{k}) = G(\mathbf{k})^{\dagger}\tilde{\mathcal{H}}(\mathbf{k})G(\mathbf{k}). \tag{C12}$$

Therefore, the eigenstate $|\tilde{\phi}_n(\mathbf{k})\rangle$ for $\tilde{\mathcal{H}}(\mathbf{k})$ is also related to the eigenstate $|\phi_n(\mathbf{k})\rangle$ for $\mathcal{H}(\mathbf{k})$ as

$$|\tilde{\phi}_n(\mathbf{k})\rangle = G(\mathbf{k})|\phi_n(\mathbf{k})\rangle. \tag{C13}$$

When $\mu_B H_z \neq 0$, $G(\mathbf{k})$ is nonsingular, thus we have

$$\begin{aligned} A_i(\mathbf{k}) &= i\sum_n \langle\phi_n(\mathbf{k})|\partial_{k_i}\phi_n(\mathbf{k})\rangle = i\sum_n \langle\tilde{\phi}_n(\mathbf{k})|\partial_{k_i}\tilde{\phi}_n(\mathbf{k})\rangle \\ &\quad - i\,\mathrm{tr}[G^{\dagger}\partial_{k_i}G(\mathbf{k})] = \tilde{A}_i(\mathbf{k}) - i\partial_{k_i}\ln[\det G(\mathbf{k})] = \tilde{A}_i(\mathbf{k}), \end{aligned} \tag{C14}$$

where we have used $\det G(\mathbf{k})=1$. Therefore, from Eq. (C11), it is found that the TKNN number remains the same in the chirality basis.

APPENDIX D: AN APPROXIMATED SOLUTION FOR THE MAJORANA ZERO-ENERGY MODE IN A VORTEX CORE

We, here, present a derivation of an approximated solution for the Majorana zero-energy mode in a vortex core considered in Sec. VII. Zero-energy solutions of the BdG

equation generally satisfy the condition $\tilde{u}_\sigma = \tilde{v}_\sigma^*$ because of the particle-hole symmetry of the BdG Hamiltonian. Thus, the BdG equation [Eq. (56)] for $E=0$ can be recast into the following two equations for $\tilde{u}_\uparrow$ and $\tilde{u}_\downarrow$:

$$\left[-\frac{1}{2m}\left(\frac{\partial^2}{\partial r^2}+\frac{1}{r}\frac{\partial}{\partial r}+\frac{1}{r^2}\frac{\partial^2}{\partial\theta^2}+i\frac{n}{r^2}\frac{\partial}{\partial\theta}-\frac{n^2}{4r^2}\right)-\mu_0-h\right]\tilde{u}_\uparrow + 2\lambda e^{-i\theta}\left(\frac{\partial}{\partial r}-\frac{i}{r}\frac{\partial}{\partial\theta}+\frac{n}{2r}\right)\tilde{u}_\downarrow+\Delta\tilde{u}_\downarrow^*=0, \tag{D1}$$

$$\left[-\frac{1}{2m}\left(\frac{\partial^2}{\partial r^2}+\frac{1}{r}\frac{\partial}{\partial r}+\frac{1}{r^2}\frac{\partial^2}{\partial\theta^2}+i\frac{n}{r^2}\frac{\partial}{\partial\theta}-\frac{n^2}{4r^2}\right)-\mu_0+h\right]\tilde{u}_\downarrow - 2\lambda e^{i\theta}\left(\frac{\partial}{\partial r}+\frac{i}{r}\frac{\partial}{\partial\theta}-\frac{n}{2r}\right)\tilde{u}_\uparrow-\Delta\tilde{u}_\uparrow^*=0. \tag{D2}$$

Here $\Delta=0$ for $r<r_c$, and $\Delta\neq 0$ for $r>r_c$ with $r_c \ll \xi$.

We first consider the solution for $r<r_c$. Then, we put $\Delta=0$ in Eqs. (D1) and (D2). We examine the following form of the solution:

$$\tilde{u}_\uparrow(r,\theta)=e^{-i(n\theta/2)}e^{i(\beta-1)\theta}f_\uparrow^<(r),\quad \tilde{u}_\downarrow(r,\theta)=e^{-i(n\theta/2)}e^{i\beta\theta}f_\downarrow^<(r). \tag{D3}$$

Here β is a constant which will be determined later. Substituting Eq. (D3) into Eqs. (D1) and (D2), we have the equations for $f_{\uparrow(\downarrow)}^<$,

$$\left[\frac{1}{2m}\left(\frac{\partial^2}{\partial r^2}+\frac{1}{r}\frac{\partial}{\partial r}-\frac{(\beta-1)^2}{r^2}\right)+\mu_0+h\right]f_\uparrow^<-2\lambda\left(\frac{\partial}{\partial r}+\frac{\beta}{r}\right)f_\downarrow^<=0, \tag{D4}$$

$$\left[\frac{1}{2m}\left(\frac{\partial^2}{\partial r^2}+\frac{1}{r}\frac{\partial}{\partial r}-\frac{\beta^2}{r^2}\right)+\mu_0-h\right]f_\downarrow^<+2\lambda\left(\frac{\partial}{\partial r}-\frac{\beta-1}{r}\right)f_\uparrow^<=0. \tag{D5}$$

We search for the solutions of Eqs. (D4) and (D5) in the form $f_\uparrow^<(r)=A_\uparrow Z_{\beta-1}(\alpha r)$ and $f_\downarrow^<(r)=A_\downarrow Z_\beta(\alpha r)$, where $Z_\nu(\alpha r)$ is the Bessel function and α is a constant. Substituting these expressions into Eqs. (D4) and (D5) and using the following relations for the Bessel functions $Z_\nu(\alpha r)$:

$$\frac{\partial Z_\nu(\alpha r)}{\partial r}=\frac{\nu}{r}Z_\nu(\alpha r)-\alpha Z_{\nu+1}(\alpha r)=\alpha Z_{\nu-1}(\alpha r)-\frac{\nu}{r}Z_\nu(\alpha r), \tag{D6}$$

we obtain

$$\left[\frac{\partial^2}{\partial r^2}+\frac{1}{r}\frac{\partial}{\partial r}-\frac{(\beta-1)^2}{r^2}+2m(\mu_0+h)-4m\lambda\alpha\frac{A_\downarrow}{A_\uparrow}\right]Z_{\beta-1}(\alpha r)=0, \tag{D7}$$

$$\left[\frac{\partial^2}{\partial r^2}+\frac{1}{r}\frac{\partial}{\partial r}-\frac{\beta^2}{r^2}+2m(\mu_0-h)-4m\lambda\alpha\frac{A_\uparrow}{A_\downarrow}\right]Z_\beta(\alpha r)=0. \tag{D8}$$

Equations (D7) and (D8) are actually the Bessel differential equations with the solutions $Z_{\beta-1}(\alpha r)$ and $Z_\beta(\alpha r)$, respectively, provided that the following relation is satisfied:

$$2m(\mu_0+h)-4m\lambda\alpha\frac{A_\downarrow}{A_\uparrow}=2m(\mu_0-h)-4m\lambda\alpha\frac{A_\uparrow}{A_\downarrow}=\alpha^2. \tag{D9}$$

α and $A_\uparrow/A_\downarrow$ are determined from Eq. (D9). For simplicity, we consider the case of $\mu_0=0$, for which one of the two SO split bands crosses the Γ point $\mathbf{k}=0$. This is a typical situation which realizes the non-Abelian topological order (and hence the Majorana zero mode) as discussed in the previous sections. We obtain two sets of solutions of Eq. (D9), (i) $\alpha=\gamma_+$, and $A_\downarrow/A_\uparrow=(\gamma_--\gamma_+)/(4m\lambda)$. (ii) $\alpha=i\gamma_-$, and $A_\downarrow/A_\uparrow=-i(\gamma_-+\gamma_+)/(4m\lambda)$.

Here $\gamma_\pm=\sqrt{\sqrt{64m^4\lambda^4+4m^2h^2}\pm 8m^2\lambda^2}$. Thus, we have two solutions of the BdG equation for $r<r_c$,

$$\tilde{u}_\uparrow=e^{-i(n\theta/2)}e^{i(\beta-1)\theta}A_\uparrow Z_{\beta-1}(\gamma_+ r),$$

$$\tilde{u}_\downarrow=e^{-i(n\theta/2)}e^{i\beta\theta}\frac{\gamma_--\gamma_+}{4m\lambda}A_\uparrow Z_\beta(\gamma_+ r)\quad \text{solution I}, \tag{D10}$$

$$\tilde{u}_\uparrow=e^{-i(n\theta/2)}e^{i(\beta-1)\theta}A_\uparrow Z_{\beta-1}(i\gamma_- r),$$

$$\tilde{u}_\downarrow=e^{-i(n\theta/2)}e^{i\beta\theta}\frac{-i}{4m\lambda}(\gamma_++\gamma_-)A_\uparrow Z_\beta(i\gamma_- r)\quad \text{solution II}. \tag{D11}$$

Note that the solution I corresponds to the contribution from electrons with the finite Fermi momentum $k_F=\gamma_+$ while the solution II is dominated by electrons in the vicinity of the Γ point $\mathbf{k}\sim 0$. In the following, we try to construct a solution for the Majorana zero-energy mode which is mainly formed by quasiparticles with $\mathbf{k}\sim 0$ corresponding to the solution II above.

We now proceed to analyze the solution of the BdG equations [Eqs. (D1) and (D2)] for $r>r_c$. The dependence on θ of the wave function can be separated by assuming the following form of the solution:

$$\tilde{u}_\uparrow(r,\theta)=e^{-i(\theta/2)}f_\uparrow^>(r),\quad \tilde{u}_\downarrow(r,\theta)=e^{i(\theta/2)}f_\downarrow^>(r). \tag{D12}$$

Since $\tilde{u}_\sigma(r,\theta)$ is multiplied by $(-1)^n$ when θ is changed from 0 to 2π in this gauge,[39] the solution [Eq. (D12)] satisfies the correct boundary condition with respect to θ only when the vorticity n is odd. Thus, we will find the zero-energy solution only for odd n.

Substituting Eq. (D12) into Eqs. (D1) and (D2), we obtain

$$\left[\frac{1}{2m}\left(\frac{\partial^2}{\partial r^2}+\frac{1}{r}\frac{\partial}{\partial r}-\frac{(n-1)^2}{4r^2}\right)+\mu_0+h\right]f_\uparrow^> - 2\lambda\left(\frac{\partial}{\partial r}+\frac{n+1}{2r}\right)f_\downarrow^>-\Delta f_\downarrow^{>*}=0, \tag{D13}$$

$$\left[\frac{1}{2m}\left(\frac{\partial^2}{\partial r^2}+\frac{1}{r}\frac{\partial}{\partial r}-\frac{(n+1)^2}{4r^2}\right)+\mu_0-h\right]f_{\downarrow}^{>}+2\lambda\left(\frac{\partial}{\partial r}-\frac{n-1}{2r}\right)f_{\uparrow}^{>}+\Delta f_{\uparrow}^{>*}=0. \tag{D14}$$

In the following, we set $\mu=0$, as mentioned before. We postulate that the solutions of Eqs. (D13) and (D14) consist of a slowly varying function of r, $g_{\uparrow(\downarrow)}(r)$ and the Bessel function; i.e.,

$$f_{\uparrow}^{>}(r)=g_{\uparrow}(r)Z_{(n-1/2)}(\alpha' r),\quad f_{\downarrow}^{>}(r)=g_{\downarrow}(r)Z_{(n+1/2)}(\alpha' r) \tag{D15}$$

with α' a constant. Substituting these expressions into Eqs. (D13) and (D14), we have

$$\frac{1}{m}\frac{\partial Z_{(n-1/2)}}{\partial r}\frac{\partial g_{\uparrow}}{\partial r}-2\lambda Z_{(n+1/2)}\frac{\partial g_{\downarrow}}{\partial r}-2\lambda\alpha' Z_{(n-1/2)}g_{\downarrow}-\Delta g_{\downarrow}^{*}Z_{(n+1/2)}^{*}+hg_{\uparrow}Z_{(n-1/2)}-\frac{\alpha'^2}{2m}g_{\uparrow}Z_{(n-1/2)}=0, \tag{D16}$$

$$\frac{1}{m}\frac{\partial Z_{n+1/2}}{\partial r}\frac{\partial g_{\downarrow}}{\partial r}-2\lambda Z_{(n-1/2)}\frac{\partial g_{\uparrow}}{\partial r}-2\lambda\alpha' Z_{(n+1/2)}g_{\uparrow}+\Delta g_{\uparrow}^{*}Z_{(n-1/2)}^{*}-hg_{\downarrow}Z_{(n+1/2)}-\frac{\alpha'^2}{2m}g_{\downarrow}Z_{(n+1/2)}=0. \tag{D17}$$

To derive the third terms of the left-hand sides of Eqs. (D16) and (D17), we have used relation (D6). We assume that the Bessel functions $Z_{\nu}(\alpha' r)$ appearing in the solution of $f_{\uparrow,\downarrow}$ are the first Hankel function $H_{\nu}^{(1)}(\alpha' r)$. To solve Eqs. (D16) and (D17) for $g_{\uparrow}$ and $g_{\downarrow}$, we use the asymptotic form of the Hankel function $H_{\nu}^{(1)}(z)\sim\sqrt{\frac{2}{\pi z}}\exp\{i[z-\frac{\pi}{4}(2\nu+1)]\}$, and the asymptotic relations,

$$\frac{1}{Z_{\nu}(\alpha' r)}\frac{\partial Z_{\nu}(\alpha' r)}{\partial r}\to i\alpha'+\frac{\nu}{r},\quad Z_{\nu-1}/Z_{\nu}\to i. \tag{D18}$$

In the following analysis, it will be revealed that the parameter α' is determined as a pure imaginary number. [See Eq. (D25).] Thus, we approximate $Z_{(n+1/2)}^{*}/Z_{(n-1/2)}\to\exp[i\frac{\pi}{2}(n+2)]$ in the asymptotic regime. Then, Eqs. (D16) and (D17) are rewritten into

$$\frac{i\alpha'}{m}\frac{dg_{\uparrow}}{dr}+2i\lambda\frac{dg_{\downarrow}}{dr}-2\lambda\alpha' g_{\downarrow}-\Delta g_{\downarrow}^{*}e^{i(\pi/2)(n+2)}+hg_{\uparrow}-\frac{\alpha'^2}{2m}g_{\uparrow}=0, \tag{D19}$$

$$\frac{i\alpha'}{m}\frac{dg_{\downarrow}}{dr}+2i\lambda\frac{dg_{\uparrow}}{dr}-2\lambda\alpha' g_{\uparrow}+\Delta g_{\uparrow}^{*}e^{i(\pi/2)(n+2)}-hg_{\downarrow}-\frac{\alpha'^2}{2m}g_{\downarrow}=0. \tag{D20}$$

We here introduce new functions $g_{\pm}(r)=g_{\uparrow}\pm ig_{\downarrow}$. From Eqs. (D19) and (D20), we have

$$\frac{i\alpha'}{m}\frac{dg_{+}}{dr}-2\lambda\frac{dg_{-}}{dr}-2i\lambda\alpha' g_{-}+i\Delta g_{-}^{*}e^{i(\pi/2)(n+2)}+hg_{-}-\frac{\alpha'^2}{2m}g_{+}=0, \tag{D21}$$

$$\frac{i\alpha'}{m}\frac{dg_{-}}{dr}+2\lambda\frac{dg_{+}}{dr}+2i\lambda\alpha' g_{+}-i\Delta g_{+}^{*}e^{i(\pi/2)(n+2)}+hg_{+}-\frac{\alpha'^2}{2m}g_{-}=0. \tag{D22}$$

To solve Eqs. (D21) and (D22), we examine the following two possible solutions: (a) $g_{-}\equiv 0$, and g_{+} gives a nontrivial solution. (b) $g_{+}\equiv 0$, and g_{-} gives a nontrivial solution.

We, first, consider the solution (a). We postulate that $g_{+}=\tilde{g}_{+}\exp[i\frac{\pi}{4}(n-1)]$ with $\tilde{g}_{+}$ a real function. Then, Eqs. (D21) and (D22) are recast into

$$\frac{d\tilde{g}_{+}}{dr}=-i\frac{\alpha'}{2}\tilde{g}_{+}, \tag{D23}$$

$$\frac{d\tilde{g}_{+}}{dr}=\left(-i\alpha'-\frac{h-\Delta}{2\lambda}\right)\tilde{g}_{+}. \tag{D24}$$

These two equations are equivalent to each other provided that

$$\alpha'=i\frac{h-\Delta}{\lambda}. \tag{D25}$$

Thus, we obtain α' as a pure imaginary, as already noticed above [below Eq. (D18)]. Therefore, the approximation used for the derivation of Eqs. (D19) and (D20) from Eqs. (D16) and (D17) is justified. Solving Eq. (D23) or Eq. (D24) with Eq. (D25), we obtain the solution for $\tilde{g}_{+}$,

$$\tilde{g}_{+}=C_{+}e^{\int^{r}dr'(h-\Delta)/2\lambda}. \tag{D26}$$

Then, from Eq. (D15), and $g_{\uparrow}=g_{+}/2$, $g_{\downarrow}=-ig_{+}/2$, we obtain the radial part of the wave functions $f_{\uparrow}^{>}$ and $f_{\downarrow}^{>}$ for the solution (a),

$$f_{\uparrow}^{>}(r)=\frac{C_{+}}{2}e^{i(\pi/4)(n-1)}e^{\int^{r}dr'(h-\Delta)/2\lambda}H_{(n+3/2)}^{(1)}\left(i\frac{h-\Delta}{\lambda}r\right), \tag{D27}$$

$$f_{\downarrow}^{>}(r)=-i\frac{C_{+}}{2}e^{i(\pi/4)(n-1)}e^{\int^{r}dr'(h-\Delta)/2\lambda}H_{(n+1/2)}^{(1)}\left(i\frac{h-\Delta}{\lambda}r\right). \tag{D28}$$

From the asymptotic form of the Hankel function $H_{\nu}^{(1)}(iar)\sim\sqrt{\frac{2}{\pi iar}}\exp[-ar-i\frac{\pi}{4}(2\nu+1)]$, we find that for large r, Eqs. (D27) and (D28) are given by

$$f_{\uparrow}^{>}(r)\sim-i\frac{C_{+}}{2}\sqrt{\frac{2\lambda}{\pi(h-\Delta)r}}e^{-[(h-\Delta)/2\lambda]r}, \tag{D29}$$

$$f_{\downarrow}^{>}(r)\sim i\frac{C_{+}}{2}\sqrt{\frac{2\lambda}{\pi(h-\Delta)r}}e^{-[(h-\Delta)/2\lambda]r}. \tag{D30}$$

Thus, these functions are normalizable when $h-\Delta>0$. We, now, consider the matching of the solution (a) for $r>r_c$ and

the solution for $r<r_c$ at $r=r_c$. As shown below, we can match the solution (a) for $r>r_c$ with the solution II for $r<r_c$ given by Eq. (D11). Putting $\beta=(n+1)/2$ and $Z_\nu(i\gamma_- r)=H_\nu^{(1)}(i\gamma_- r)$ in Eq. (D11), we find the asymptotic behaviors of the radial part of the solution II for $r<r_c$,

$$f_\uparrow^<(r)=A_\uparrow H_{(n-1/2)}^{(1)}(i\gamma_- r)\sim A_\uparrow e^{-i(\pi/4)(n+1)}\sqrt{\frac{2}{\pi\gamma_- r}}e^{-\gamma_- r}, \tag{D31}$$

$$f_\downarrow^<(r)=A_\downarrow H_{(n+1/2)}^{(1)}(i\gamma_- r)\sim -iA_\downarrow e^{-i(\pi/4)(n+1)}\sqrt{\frac{2}{\pi\gamma_- r}}e^{-\gamma_- r}. \tag{D32}$$

To match the solutions, we adopt the following approximation. Assuming that the SO split is much larger than the Zeeman energy, i.e., $h\ll m\lambda^2$, we have $\gamma_-\approx h/(2\lambda)$, $A_\downarrow/A_\uparrow=-i(\gamma_+ +\gamma_-)/(4m\lambda)\approx -i$. Then, noting that $\Delta\to 0$ at $r\sim r_c$, we can match the solution for $r>r_c$, Eqs. (D29) and (D30), with the solution for $r<r_c$, Eqs. (D31) and (D32), by choosing $C_+=2\sqrt{2}i\exp[-i\frac{\pi}{4}(n+1)]A_\uparrow$. The solution for $r<r_c$, Eqs. (D31) and (D32), is not regular at $r=0$, exhibiting logarithmic divergence $\sim\log(r)$ for $r\to 0$. However, the solution is still normalizable. Thus, the solution (a) for $r>r_c$ and the solution II for $r<r_c$ constitute the normalizable solution for the Majorana zero-energy mode. This Majorana zero-energy solution is constructed from quasiparticles in the vicinity of the Γ point $\mathbf{k}\sim 0$, i.e., a single Dirac cone with a mass gap $\sim h$, as mentioned before.

We, now, examine the solution (b) for $r>r_c$; i.e., $g_+=0$, and g_- gives a nontrivial solution. In this case, we assume the solution of the form $g_-(r)=\exp[i\frac{\pi}{4}(n+1)]\tilde{g}_-(r)$ with $\tilde{g}_-(r)$ a real function. Then, Eqs. (D21) and (D22) are recast in

$$\frac{d\tilde{g}_-}{dr}=-i\frac{\alpha'}{2}\tilde{g}_-, \tag{D33}$$

$$\frac{d\tilde{g}_-}{dr}=\left(-i\alpha'+\frac{h-\Delta}{2\lambda}\right)\tilde{g}_-. \tag{D34}$$

These two equations are equivalent when

$$\alpha'=i\frac{\Delta-h}{\lambda}. \tag{D35}$$

For this choice of α', the radial part of the solution (b) is given by

$$f_\uparrow^>(r)=\frac{C_-}{2}e^{i(\pi/4)(n+1)}e^{-\int^r dr'(h-\Delta)/2\lambda}Z_{(n-1/2)}\left(i\frac{\Delta-h}{\lambda}r\right), \tag{D36}$$

$$f_\downarrow^>(r)=i\frac{C_-}{2}e^{i(\pi/4)(n+1)}e^{-\int^r dr'(h-\Delta)/2\lambda}Z_{(n+1/2)}\left(i\frac{\Delta-h}{\lambda}r\right). \tag{D37}$$

We cannot match Eqs. (D36) and (D37) with the solution for $r<r_c$ at $r\sim r_c$ for any choice of the Bessel function $Z_\nu[i(\Delta-h)r/\lambda]$.

Thus, when $h>\Delta$ and the vorticity n is odd, we obtain the only one normalizable zero-energy solution which is given by Eqs. (D12), (D27), and (D28) for $r>r_c$, and Eq. (D11) for $r<r_c$ with $\beta=(n+1)/2$ and $Z_\nu=H_\nu^{(1)}$. The field operator for the zero-energy mode is given by $\gamma^\dagger=\int d\mathbf{r}[\tilde{u}_\uparrow(\mathbf{r})c_\uparrow^\dagger(\mathbf{r})+\tilde{u}_\downarrow(\mathbf{r})c_\downarrow^\dagger(\mathbf{r})+\tilde{u}_\uparrow^*(\mathbf{r})c_\uparrow(\mathbf{r})+\tilde{u}_\downarrow^*(\mathbf{r})c_\downarrow(\mathbf{r})]$, which is self-Hermitian. Thus, the zero-energy mode is a Majorana fermion. There is only one Majorana fermion mode in a vortex core with odd vorticity for $h>\Delta$.

APPENDIX E: NON-ABELIAN ANYON IN A TIME-REVERSAL INVARIANT *s*-WAVE SUPERCONDUCTING STATE: NON-ABELIAN AXION STRING (REF. 24) AND THE FU-KANE MODEL (REF. 23)

In this paper, we mainly consider spin-singlet superconducting states under strong Zeeman magnetic field. Thus the time-reversal symmetry is explicitly broken in the ground state. Indeed, the time-reversal breaking is necessary to obtain a nonzero TKNN number. From the bulk-edge correspondence, the nonzero TKNN number ensures the existence of topologically stable gapless Majorana fermions on a boundary and Majorana zero modes on a vortex.

However, it has been also known that non-Abelian anyons can be realized even when the ground state does not break the time-reversal invariance. Because of the time-reversal invariance, the TKNN number in this case is trivially zero. Nevertheless, the index theorem ensures the existence of a topologically stable Majorana zero mode in a vortex. This mechanism of non-Abelian anyon was discussed in Ref. 24. Recently, Fu and Kane pointed out that Majorana fermions (and hence, non-Abelian anyons) realize in an interface between a topological insulator and an *s*-wave superconductors which preserves time-reversal symmetry.[23] The following analysis presents a general ground for the realization of non-Abelian anyons in such time-reversal invariant systems.

To see this, consider the following Lagrangian for a 2+1-dimensional Majorana fermion ψ_{M} coupled with an scalar field $\Phi=\Phi_1+\Phi_2$:[24]

$$\mathcal{L}=\frac{i}{2}\psi_{\mathrm{M}}^\dagger\gamma^0\gamma^\mu\partial_\mu\psi_{\mathrm{M}}-\frac{1}{2}\psi_{\mathrm{M}}^\dagger\gamma^0(\Phi_1+i\gamma_5\Phi_2)\psi_{\mathrm{M}}. \tag{E1}$$

Here the Majorana fermion satisfies the Majorana condition,

$$i\gamma_2\psi_{\mathrm{M}}^*=\psi_{\mathrm{M}} \tag{E2}$$

and the Dirac gamma matrices γ^μ and γ_5 are given by

$$\gamma^\mu=\begin{pmatrix}0 & \sigma^\mu\\ \bar{\sigma}^\mu & 0\end{pmatrix},\quad \gamma_5=\begin{pmatrix}1 & 0\\ 0 & -1\end{pmatrix}, \tag{E3}$$

where $\sigma^\mu=(1,-\sigma_i)$ and $\bar{\sigma}^\mu=(1,\sigma_i)$ with the Pauli matrices σ_i. We also suppose that Φ is an *s*-wave condensate with the expectation value $\langle\Phi\rangle=\Phi_0$. In sharp contrast to other non-Abelian topological phases, the system is time-reversal invariant, as was pointed out in Ref. 24.

The above system has the following $U(1)$ symmetry:

$$\psi_{\mathrm{M}}\to e^{i\gamma_5\theta}\psi_{\mathrm{M}},\quad \Phi\to e^{-2\theta}\Phi, \tag{E4}$$

which is spontaneously broken by the condensate Φ_0. Therefore, like an ordinary *s*-wave superconducting state, there

exist a stable vortex solution that is given by

$$\Phi(\mathbf{x}) = \Phi_0 f(\rho) e^{i\varphi}, \tag{E5}$$

where ρ and ϕ are the radial and angular coordinates from the vortex, respectively. The function $f(\rho)$ vanishes on the core of the vortex and approaches to $f(\infty)=1$ far away from the core.

The bound states in a vortex are studied by using the Hamiltonian of the system,

$$\mathcal{H} = \begin{pmatrix} -i\sigma_i\partial_i & \Phi^* \\ \Phi^* & i\sigma_i\partial_i \end{pmatrix} \tag{E6}$$

and the unique zero mode, which satisfies $\mathcal{H}u_0=0$, is given by

$$u_0 = C\begin{pmatrix} 0 \\ 1+i \\ 1-i \\ 0 \end{pmatrix} \exp\left[-\Phi_0 \int_0^\rho dr f(r)\right] \tag{E7}$$

with a normalization constant C.[64,65] The topological stability of the zero mode is ensured by the index theorem.[66] From the Majorana condition Eq. (E2) in 2+1 dimensions, the operator of the zero mode $\gamma=\int d\mathbf{x} u_0^\dagger(\mathbf{x})\psi_M(\mathbf{x})$ becomes real, i.e., $\gamma^\dagger=\gamma$. Therefore, the vortex obeys the non-Abelian statistics.

The above mechanism of non-Abelian anyons in an s-wave superconducting state is applicable to axion strings in cosmological systems,[24] and also to an interface between a topological insulator and an s-wave superconductor considered by Fu and Kane.[23] Indeed, identifying a gapless Dirac fermion on a surface of the topological insulator in the Nambu representation $(\psi_\uparrow,\psi_\downarrow,\psi_\downarrow^\dagger,-\psi_\uparrow^\dagger)$ and an s-wave Cooper pair due to the proximity effect with the Majorana field ψ_M and the scalar field Φ, respectively, one can show that the BdG Hamiltonian considered in Ref. 23 is essentially the same as Hamiltonian (E6). In this identification, the Dirac fermion in the Nambu representation satisfies the Majorana condition [Eq. (E2)] up to an unimportant factor. Furthermore, the electromagnetic $U(1)$ gauge symmetry in the Fu-Kane model reduces to the $U(1)$ axial symmetry [Eq. (E4)]. Therefore, for the same reason mentioned above, a vortex in the Fu-Kane model is found to obey the non-Abelian anyon statistics.

[1] X. G. Wen and Q. Niu, Phys. Rev. B **41**, 9377 (1990).
[2] X. G. Wen, Phys. Rev. Lett. **64**, 2206 (1990).
[3] G. Moore and N. Read, Nucl. Phys. B **360**, 362 (1991).
[4] C. Nayak and F. Wilczek, Nucl. Phys. B **479**, 529 (1996).
[5] N. Read and D. Green, Phys. Rev. B **61**, 10267 (2000).
[6] D. A. Ivanov, Phys. Rev. Lett. **86**, 268 (2001).
[7] M. Stone and S.-B. Chung, Phys. Rev. B **73**, 014505 (2006).
[8] A. Stern, F. von Oppen, and E. Mariani, Phys. Rev. B **70**, 205338 (2004).
[9] M. Stone and R. Roy, Phys. Rev. B **69**, 184511 (2004).
[10] A. P. Schnyder, S. Ryu, A. Furusaki, and A. W. W. Ludwig, Phys. Rev. B **78**, 195125 (2008).
[11] G. E. Volovik, Phys. Rep. **351**, 195 (2001).
[12] M. Freedman, A. Kitaev, M. Larsen, and Z. Wang, Bull. Am. Math. Soc. **40**, 31 (2003).
[13] A. Kitaev, Ann. Phys. **303**, 2 (2003).
[14] S. Das Sarma, M. Freedman, and C. Nayak, Phys. Rev. Lett. **94**, 166802 (2005).
[15] N. Read and E. Rezayi, Phys. Rev. B **59**, 8084 (1999).
[16] N. B. Kopnin and M. M. Salomaa, Phys. Rev. B **44**, 9667 (1991).
[17] S. Tewari, S. Das Sarma, C. Nayak, C. Zhang, and P. Zoller, Phys. Rev. Lett. **98**, 010506 (2007).
[18] C. Zhang, S. Tewari, R. M. Lutchyn, and S. Das Sarma, Phys. Rev. Lett. **101**, 160401 (2008).
[19] Y. Tsutsumi, T. Kawakami, T. Mizushima, M. Ichioka, and K. Machida, Phys. Rev. Lett. **101**, 135302 (2008).
[20] N. R. Cooper and G. V. Shlyapnikov, Phys. Rev. Lett. **103**, 155302 (2009).
[21] M. Sato and S. Fujimoto, Phys. Rev. B **79**, 094504 (2009).
[22] M. Sato, Phys. Rev. B **81**, 220504(R) (2010).
[23] L. Fu and C. L. Kane, Phys. Rev. Lett. **100**, 096407 (2008).
[24] M. Sato, Phys. Lett. B **575**, 126 (2003).
[25] In contrast to other non-Abelian topological phases, the systems considered in Refs. 23 and 24 do not break the time-reversal invariance in the ground state. Thus the Chern number is trivially zero. Nevertheless, the index theorem ensures the existence of a topologically stable Majorana zero mode in a vortex, which implies that the vortices obey the non-Abelian statistics. See Appendix E.
[26] M. Sato, Y. Takahashi, and S. Fujimoto, Phys. Rev. Lett. **103**, 020401 (2009); e-print arXiv:0901.4693v1 (unpublished).
[27] J. D. Sau, R. M. Lutchyn, S. Tewari, and S. Das Sarma, Phys. Rev. Lett. **104**, 040502 (2010).
[28] J. Alicea, Phys. Rev. B **81**, 125318 (2010).
[29] M. Cheng, R. M. Lutchyn, V. Galitski, and S. Das Sarma, Phys. Rev. Lett. **103**, 107001 (2009).
[30] E. I. Rashba, Sov. Phys. Solid State **2**, 1109 (1960).
[31] V. M. Edelstein, Sov. Phys. JETP **68**, 1244 (1989).
[32] L. P. Gor'kov and E. I. Rashba, Phys. Rev. Lett. **87**, 037004 (2001).
[33] P. A. Frigeri, D. F. Agterberg, A. Koga, and M. Sigrist, Phys. Rev. Lett. **92**, 097001 (2004).
[34] S. Fujimoto, J. Phys. Soc. Jpn. **76**, 034712 (2007).
[35] S. Fujimoto, J. Phys. Soc. Jpn. **76**, 051008 (2007).
[36] M. Sato, Phys. Rev. B **73**, 214502 (2006).
[37] The argument here was first outlined in the preprint version of Ref. 26.
[38] Note that the definition of the Chern number in Ref. 26 is different from the TKNN number in this paper by a factor −1.
[39] C. Caroli, P. G. de Gennes, and J. Matricon, Phys. Lett. **9**, 307 (1964).
[40] J. Sau, R. Lutchyn, S. Tewari, and S. Das Sarma, arXiv:0912.4508 (unpublished).
[41] A. R. Akhmerov, J. Nilsson, and C. W. J. Beenakker, Phys. Rev. Lett. **102**, 216404 (2009).

[42] W. P. Su, J. R. Schrieffer, and A. J. Heeger, Phys. Rev. B **22**, 2099 (1980).
[43] R. Jackiw and C. Rebbi, Phys. Rev. D **13**, 3398 (1976).
[44] K. Izawa, Y. Kasahara, Y. Matsuda, K. Behnia, T. Yasuda, R. Settai, and Y. Onuki, Phys. Rev. Lett. **94**, 197002 (2005).
[45] I. Bonalde, W. Bramer-Escamilla, and E. Bauer, Phys. Rev. Lett. **94**, 207002 (2005).
[46] N. Kimura, K. Ito, K. Saitoh, Y. Umeda, H. Aoki, and T. Terashima, Phys. Rev. Lett. **95**, 247004 (2005).
[47] I. Sugitani *et al.*, J. Phys. Soc. Jpn. **75**, 043703 (2006).
[48] H. Mukuda, T. Fujii, T. Ohara, A. Harada, M. Yashima, Y. Kitaoka, Y. Okuda, R. Settai, and Y. Onuki, Phys. Rev. Lett. **100**, 107003 (2008).
[49] Y. Tada, N. Kawakami, and S. Fujimoto, Phys. Rev. Lett. **101**, 267006 (2008).
[50] T. Bourdel, L. Khaykovich, J. Cubizolles, J. Zhang, F. Chevy, M. Teichmann, L. Tarruell, S. J. J. M. F. Kokkelmans, and C. Salomon, Phys. Rev. Lett. **93**, 050401 (2004).
[51] J. K. Chin, D. E. Miller, Y. Liu, C. Stan, W. Setiawan, C. Sanner, K. Xu, and W. Ketterle, Nature (London) **443**, 961 (2006).
[52] K. Osterloh, M. Baig, L. Santos, P. Zoller, and M. Lewenstein, Phys. Rev. Lett. **95**, 010403 (2005).
[53] J. Ruseckas, G. Juzeliunas, P. Ohberg, and M. Fleischhauer, Phys. Rev. Lett. **95**, 010404 (2005).
[54] S. L. Zhu, H. Fu, C. J. Wu, S. C. Zhang, and L. M. Duan, Phys. Rev. Lett. **97**, 240401 (2006).
[55] T. D. Stanescu, C. Zhang, and V. Galitski, Phys. Rev. Lett. **99**, 110403 (2007).
[56] D. Jaksch and P. Zoller, New J. Phys. **5**, 56 (2003).
[57] E. Fradkin, C. Nayak, A. Tsvelik, and F. Wilczek, Nucl. Phys. B **516**, 704 (1998).
[58] W. J. Hossack, E. Theofanidou, J. Crain, K. Heggarty, and M. Birch, Opt. Express **11**, 2053 (2003).
[59] B. Kumar and B. S. Shastry, Phys. Rev. B **68**, 104508 (2003).
[60] Q. H. Wang, D. H. Lee, and P. A. Lee, Phys. Rev. B **69**, 092504 (2004).
[61] M. Sato, Phys. Rev. B **79**, 214526 (2009).
[62] X. L. Qi, T. L. Hughes, and S. C. Zhang, Phys. Rev. B **78**, 195424 (2008).
[63] S. Fujimoto, Phys. Rev. B **77**, 220501(R) (2008).
[64] R. Jackiw and P. Rossi, Nucl. Phys. B **190**, 681 (1981).
[65] C. G. Callan, Jr. and J. A. Harvey, Nucl. Phys. B **250**, 427 (1985).
[66] G. W. Semenoff, Phys. Rev. D **37**, 2838 (1988).